



Volker ARENDT

# **Geometry and kinematics of the Theo Jansen mechanism**

## **Diploma Thesis**

to achieve the university degree of

Magister der Naturwissenschaften

Master's degree programme: Lehramt Geometrie

submitted to

**Graz University of Technology**

Supervisor

Gfrerrer, Anton, Ao.Univ.-Prof. Mag.rer.nat. Dr.techn.

Institute for Geometry

Graz, June 2019

## Affidavit

I declare that I have authored this thesis independently, that I have not used other than the declared sources/resources, and that I have explicitly indicated all material which has been quoted either literally or by content from the sources used. The text document uploaded to TUGRAZonline is identical to the present master's thesis.

---

Date

---

Signature

## Acknowledgments

First and foremost I would like to thank everyone who supported me directly or indirectly in writing this thesis.

Further I am grateful to Anton Gfrerrer for the scientific supervision of my work. His impetuses and suggestions made an enormous contribution to the present thesis.

I would particularly like to thank my family, who supported me financially and morally and always made it possible for me to pursue my goals and complete my studies. Special thanks to Sandra who kept me motivated during this process. I would also like to express my gratitude to Joy and Paul Reed, who fostered my love for English and thus encouraged me to write this thesis in English.

## Abstract

This thesis aims to analyze the one parametric motion of the Jansen mechanism. A genetic algorithm is developed and tested to generate mechanisms close or similar to the Jansen mechanism.

For this purpose the achievements by Theo Jansen are introduced. Later on a four bar linkage is used as an example to apply the kinematic fundamentals. The results are transferred to the Jansen mechanism and an instantaneous center of revolution configuration of the mechanism is illustrated. To visualize the mechanism and calculate its positions a parametrization of the Jansen mechanism is presented.

The parametrization is further used to synthesize mechanisms of the same architecture as the Jansen mechanism with a genetic algorithm. The main focus of this part is on generating a working starting population for the algorithm. The genetic part of the algorithm is described in great detail. The results of the algorithm can be categorized into four groups, which are presented with many figures in the last part of this thesis.

# Contents

<b>Abstract</b>	<b>iv</b>
<b>I. Fundamentals</b>	<b>1</b>
<b>1. Introduction</b>	<b>2</b>
1.1. Theo Jansen	2
1.2. The Jansen mechanism	5
1.2.1. Evolutionary method	5
1.2.2. Twelve holy numbers	5
<b>2. Kinematical fundamentals</b>	<b>7</b>
2.1. Transformations in the plane	7
2.2. One parameter motions in the plane	8
2.3. Velocities of planar motions	9
2.3.1. Velocity vector of a point	10
2.3.2. Velocity distribution	10
2.4. Mechanisms	11
2.5. Example four bar linkage	13
<b>3. Analysis of the Jansen mechanism</b>	<b>22</b>
3.1. Description of the Jansen mechanism	22
3.2. ICR configuration of the Jansen mechanism	24
3.3. Geometrical analysis of the velocities of the Jansen mechanism	28
3.4. Parametrization of the Jansen mechanism	32
<b>II. Optimization</b>	<b>36</b>
<b>4. Optimization of the Jansen mechanism</b>	<b>37</b>
4.1. Introduction to genetic algorithms	37
4.2. Genetic algorithm for synthesizing a Jansen-style mechanism	38
4.2.1. Starting population	41
4.2.2. Selection, recombination, mutation and replacement	51

## Contents

4.2.3. End of algorithm . . . . .	52
<b>5. Results of the genetic algorithm</b>	<b>54</b>
5.1. Results close to the Jansen mechanism . . . . .	55
5.1.1. Further results close to the Jansen mechanism . . . . .	62
5.2. Inverse mechanisms . . . . .	63
5.2.1. Further inverse results . . . . .	67
5.3. Mixed mechanisms . . . . .	68
5.3.1. Further mixed results . . . . .	72
5.4. Infeasible mechanisms . . . . .	73
<b>6. Conclusion</b>	<b>74</b>
<b>References</b>	<b>76</b>

# List of Figures

1.1.	Portrait Theo Jansen . . . . .	2
1.2.	Leg <i>Animaris Vulgaris</i> . . . . .	4
1.3.	Leg <i>Animaris Currens Vulgaris</i> . . . . .	4
1.4.	Jansen's ideal locus . . . . .	5
1.5.	Notations Jansen mechanism (JM) . . . . .	6
2.1.	Rotational center of two lines . . . . .	7
2.2.	Proper isometries are not commutative . . . . .	8
2.3.	One parameter motion in the plane . . . . .	9
2.4.	Velocity distribution of instantaneous revolution . . . . .	11
2.5.	Velocity distribution of instantaneous translation . . . . .	11
2.6.	Revolute joint . . . . .	12
2.7.	ICR of four bar linkage (FBL) . . . . .	14
2.8.	Velocity distribution of FBL . . . . .	15
2.9.	Notations of FBL . . . . .	16
2.10.	Coordinate frames of FBL . . . . .	20
3.1.	Systems of JM . . . . .	22
3.2.	ICR of second FBL of JM . . . . .	25
3.3.	ICR of first and second FBL of JM . . . . .	26
3.4.	ICR of third FBL of JM . . . . .	27
3.5.	ICR end-effector base of JM . . . . .	29
3.6.	ICR of JM . . . . .	30
3.7.	Velocity distribution of JM . . . . .	31
3.8.	Notation of JM for parametrization . . . . .	33
4.1.	Notation of genes of Jansen-style mechanism . . . . .	40
4.2.	Minimum of the angle $\theta$ . . . . .	44
4.3.	Maximum of the angle $\theta$ . . . . .	45
4.4.	Restrictions of third FBL in the GA . . . . .	46
4.5.	Parameters $i, j$ - Step 1 . . . . .	47
4.6.	Parameters $i, j$ - Step 2 . . . . .	47
4.7.	Parameters $i, j$ - Step 3 . . . . .	49
4.8.	Parameters $i, j$ - Step 4 . . . . .	50
4.9.	Two point crossover . . . . .	52

## List of Figures

4.10. Flowchart of the genetic algorithm . . . . .	53
5.1. Animation of the Jansen mechanism . . . . .	55
5.2. Error reduction of genetic algorithm . . . . .	56
5.3. Evolving of a mechanism through generations . . . . .	57
5.4. Generated Jansen-style mechanism . . . . .	59
5.5. Animation of the new mechanism in comparison to the Jansen mechanism . . . . .	60
5.6. Animation of the generated mechanism . . . . .	61
5.7. Generated inverse mechanism . . . . .	64
5.8. Animation of the inverse mechanism in comparison to the Jansen mechanism . . . . .	65
5.9. Animation of the generated inverse mechanism . . . . .	66
5.10. Generated mixed mechanism . . . . .	69
5.11. Animation of the mixed mechanism in comparison to the Jansen mechanism . . . . .	70
5.12. Animation of the mixed mechanism . . . . .	71
5.13. Generated infeasible mechanism . . . . .	73
6.1. Percentage of the produced types of mechanisms . . . . .	74

**Part I.**  
**Fundamentals**

# 1. Introduction

## 1.1. Theo Jansen



Figure 1.1.: Portrait of Theo Jansen , [6, p. 02.08.2018]

1948	born in Scheveningen, Netherlands
1974 – present	numerous exhibitions around the globe
1975	stops studying physics to become an artist
1980	flies UFO across Delft, Netherlands
1990 – present	develops Animari (beach animals)
2005	wins special prize of the Jury of Prix Ars Electronica in Linz, Austria [4, p. 503]

Table 1.1.: Biography of Theo Jansen ([3, p. 239])

## 1. Introduction

According to his Book [3], Theo Jansen was born in the town Scheveningen in the Netherlands in 1948. He began studying physics but stopped his studies to become an artist. Jansen states out that there is always an engineer and an artist way of working. Since most of the engineers use the same methods the constructions usually work perfectly, but they all seem to be similar. As an artist the methods are more versatile and at the beginning many artists do not know what they will have at the end. Jansen set his life goal to create a *living* life form. He recognized, that any living creature is basically made up of proteins, and therefore he only uses one material in multiple ways. Even before the year 1990 Jansen had the idea of creating walking creatures, which he called *Quadrupes*. These were boxes with four legs which could theoretically move back and forth. Jansen implemented these creatures in the computer and at that point the movement of the legs was random. Jansen created more than 200 *Quadrupes* and calculated the walking speed, if there even was any movement, of each creature. He copied the details of the fastest *Quadrupes* and used their geometry as a base for the next generation. Within the fifth generation, the *Quadrupes* were actually walking and even galloping at some occasions. Jansen was working with plastic tubes, which are still used to conduct electricity in Dutch houses and found out that there are many ways of using these tubes. Jansen spent a whole year just experimenting and learning how to use the tubes. The tubes reminded him of proteins which could have different functions.

Jansen gives a unique name to each animal that he creates and they can all be placed in an phylogenetic tree. In the year 1990 the *Animaris Vulgaris* was born to be the first walking animal. The mechanism was not able to lift a leg and move it forward, but it could turn its ankle, so that the foot was dragged (see Fig. 1.2). There were actually two cranks that drove the mechanism, which were mounted with a constant angle of  $90^\circ$ . Jansen was working with legs instead of wheels, because they work better in sand. For a creature to walk without jumping it is necessary that the fixed pivotal points have a constant distance to the ground. Unfortunately the animal did not move at all, because the adhesive tape that Jansen was using for connections at that time, was not strong enough to carry the whole construction.

The next generation of animal was the *Animaris Currens Vulgaris*, which was the first animal to stand and walk on its own. Jansen changed from using tape to using cable ties. In addition, he managed to simplify the leg mechanism so that it was only driven by a single crank. One night he had the idea to use a computer program to calculate the length of the bars needed to achieve his goal (see Fig. 1.3).

## 1. Introduction

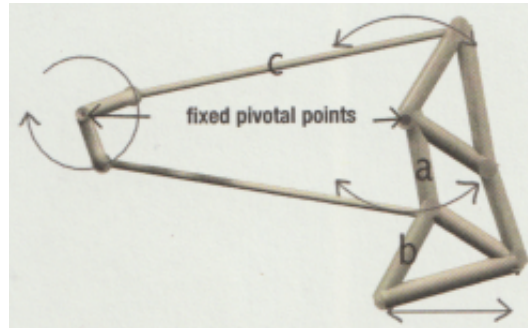


Figure 1.2.: Leg of *Animaris Vulgaris*, [3, p. 41]

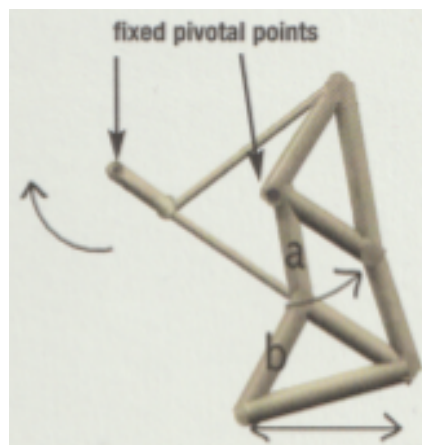


Figure 1.3.: Leg of *Animaris Currens Vulgaris*, [3, p. 51]

## 1.2. The Jansen mechanism

### 1.2.1. Evolutionary method

Jansen knew that the locus for a walking mechanism has to have a special shape without corners. The base should be its longest side, that is where the foot touches the ground. The upper part can be moved through faster to reach the beginning of the next step (see Fig. 1.4). Small variations in the length of each bar of a mechanism can cause big changes in the locus and the velocity distribution along it, so Jansen decided to approach the problem using an evolutionary method.

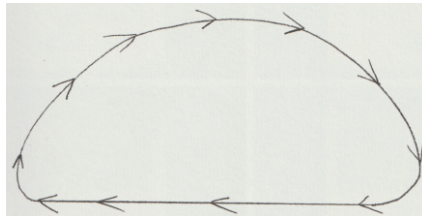


Figure 1.4.: Jansen's ideal locus of a leg mechanism, [3, p. 55]

### 1.2.2. Twelve holy numbers

Jansen set up a program to calculate the loci of 1500 legs and compared the outcome. He then chose the best 100 of these legs and constructed 1500 new legs, by combining the most convincing ones. With every generation of legs he came closer to the desired results. After his program had run for a few months, it returned a set of lengths for the twelve bars of his mechanism. Theo Jansen called those numbers the *twelve holy numbers*.

Whenever a foot is lifted, it does not support the animal, so at that moment there is no use for that foot. Therefore keeping that time as short as possible was one criterion to consider when creating the new generation of legs. One other criterion which Jansen used was that the base of the locus is getting moved through with an approximately constant velocity as long as possible. In Figure 1.5 the notation of the bars which Jansen used can be seen.

## 1. Introduction

The twelve holy numbers are  
 $a = 38$ ,  $b = 41.5$ ,  $c = 39.3$ ,  $d = 40.1$ ,  $e = 55.8$ ,  $f = 39.4$ ,  
 $g = 36.7$ ,  $h = 65.7$ ,  $i = 49$ ,  $j = 50$ ,  $k = 61.9$ ,  $l = 7.8$   
and the length of the crank  $m = 15$

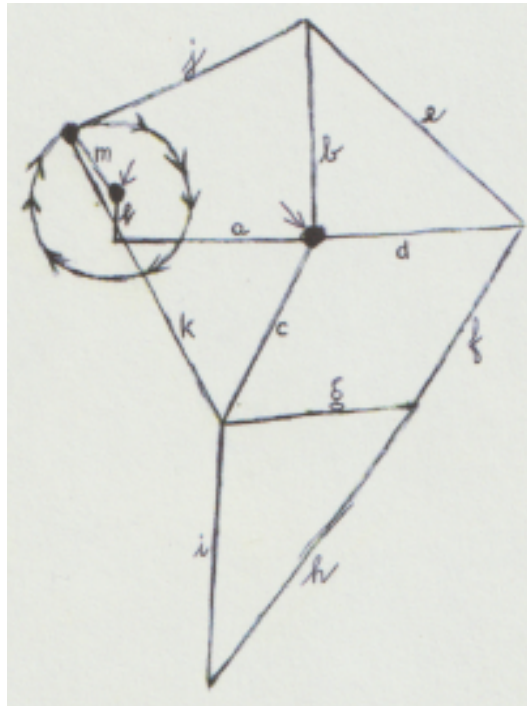


Figure 1.5.: Notation of the individual bars of the Jansen mechanism, [3, p. 57]

## 2. Kinematical fundamentals

### 2.1. Transformations in the plane

**Definition 1** (Proper isometries). [2, p. 1]

The *euclidean plane*  $\mathbb{E}_2$  is the affine plane equipped with an euclidean metric. A distance-preserving mapping  $\kappa$  for points in the euclidean plane is called an *isometry*. If the map also preserves the orientation of any triangle, the mapping is called a *proper isometry*.

**Theorem 1** (Fundamental theorem of plane kinematics). [7, p. 14-15]

Any proper isometry is either a rotation or a translation (see Fig. 2.1).

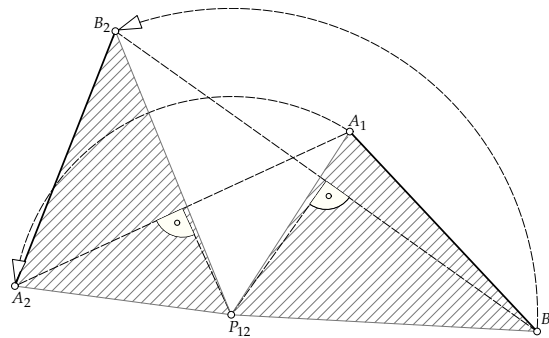


Figure 2.1.: Center of revolution of two lines

Translations with translation vector  $\mathbf{v}$  and rotations  $(M, \varphi)$  around a point  $M$  with an angle  $\varphi$  are two examples for proper isometries. In general, the composition of a rotation and a translation do not commute (see Fig.: 2.2).

Any proper isometry  $\kappa$  in the plane can be described as follows:

$$\begin{pmatrix} x_0 \\ y_0 \end{pmatrix} = \begin{pmatrix} d_x \\ d_y \end{pmatrix} + \mathbf{R} \cdot \begin{pmatrix} x_1 \\ y_1 \end{pmatrix} = \mathbf{d} + \mathbf{R} \cdot \mathbf{x}_1. \quad (2.1)$$

with

$$\mathbf{d} = \begin{pmatrix} d_x \\ d_y \end{pmatrix} \quad \text{and} \quad \mathbf{R} = \begin{pmatrix} \cos(\varphi) & -\sin(\varphi) \\ \sin(\varphi) & \cos(\varphi) \end{pmatrix}.$$

## 2. Kinematical fundamentals

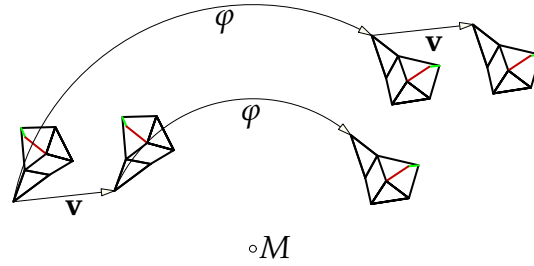


Figure 2.2.: In general a translation and a revolution are not commutative.

The same transformation can be written as

$$\begin{pmatrix} 1 \\ x_0 \\ y_0 \end{pmatrix} = \underbrace{\begin{pmatrix} 1 & 0 & 0 \\ d_x & \cos(\varphi) & -\sin(\varphi) \\ d_y & \sin(\varphi) & \cos(\varphi) \end{pmatrix}}_{\mathbf{M}} \begin{pmatrix} 1 \\ x_1 \\ y_1 \end{pmatrix} = \begin{pmatrix} 1 & \mathbf{o}^T \\ \mathbf{d} & \mathbf{R} \end{pmatrix} \begin{pmatrix} 1 \\ \mathbf{x}_1 \end{pmatrix}. \quad (2.2)$$

With 2.2 there exists a unique matrix  $\mathbf{M}$  for each proper isometry and for the composition of proper isometries these matrices can be multiplied.

## 2.2. One parameter motions in the plane

**Definition 2** (One parameter motion). [2, p. 4]

A one parameter set of proper isometries in the plane is called a *one parameter planar motion*.

The parameter  $t$  is interpreted as time. A visualization of a one parameter planar motion is moving around a sheet of paper on a table. The table is called the *fixed system*  $\Sigma_0$  and the paper the *moving system*  $\Sigma_1$ . Any point  $X \in \Sigma_1$  describes a path  $b_X$  in  $\Sigma_0$  (see Fig. 2.3).

A one parameter motion can be written as

$$\Sigma_1 \setminus \Sigma_0 : \mathbf{x}_0 = \mathbf{d}(t) + \mathbf{R}(t) \cdot \mathbf{x}_1. \quad (2.3)$$

There are two possible ways to interpret 2.3:

1. The equation can be read as two coordinate frames describing one and the same point  $X$ . There is a coordinate frame  $F_0 = \{O_0, \mathbf{e}_{01}, \mathbf{e}_{02}\}$  in  $\Sigma_0$

## 2. Kinematical fundamentals

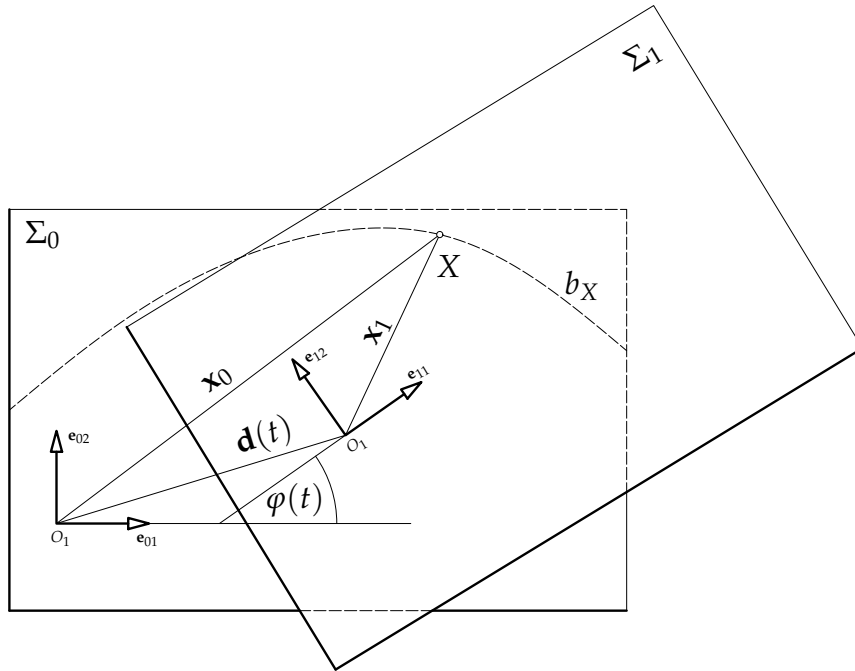


Figure 2.3.: One parameter motion in the plane

and another one  $F_1 = \{O_1, \mathbf{e}_{11}, \mathbf{e}_{12}\}$  in  $\Sigma_1$ .  $\mathbf{x}_0 = \begin{pmatrix} x_0 \\ y_0 \end{pmatrix}$  and  $\mathbf{x}_1 = \begin{pmatrix} x_1 \\ y_1 \end{pmatrix}$  are the coordinate columns of a point  $X$  with respect to  $F_0$  and  $F_1$ , respectively.

2. On the other hand, the two vectors  $\mathbf{x}_0 = \begin{pmatrix} x_0 \\ y_0 \end{pmatrix}$  and  $\mathbf{x}_1 = \begin{pmatrix} x_1 \\ y_1 \end{pmatrix}$  can also be considered as coordinate columns of two distinct points  $X_0$  and  $X_1$  with respect to one fixed coordinate frame:  $X_0$  is the original point and  $X_1$  the displaced one.

Hereinafter the first interpretation of 2.3 will be used. The only exception will be when we derive the dependencies of the angles of a four bar mechanism (see subsection 2.5).

### 2.3. Velocities of planar motions

An interesting aspect of any one parameter motion is the velocity distribution of the points  $X \in \Sigma_1$  at a particular time instance  $t$ .

## 2. Kinematical fundamentals

### 2.3.1. Velocity vector of a point

For a given one parameter motion as described in 2.3 the velocity  $\mathbf{v}_X$  of any point  $X \dots \mathbf{x}_1 = \begin{pmatrix} x_1 \\ y_1 \end{pmatrix}$  represented with respect to the coordinate frame in  $\Sigma_1$  can be calculated by deriving 2.3.

$$\mathbf{v}_X = \dot{\mathbf{x}}_0 = \dot{\mathbf{d}} + \dot{\mathbf{R}} \mathbf{x}_1 \quad (2.4)$$

$$= \dot{\mathbf{d}} + \underbrace{\dot{\mathbf{R}} \mathbf{R}^T}_{=: \mathbf{W}} \cdot (\mathbf{x}_0 - \mathbf{d}) \quad (2.5)$$

$\mathbf{R}$  is an orthogonal matrix and therefore  $\mathbf{R}^T = \mathbf{R}^{-1}$ . The matrix  $\mathbf{W}$  is called the *angular velocity matrix*. It is easy to check that

$$\mathbf{W} = \begin{pmatrix} 0 & -\dot{\varphi} \\ \dot{\varphi} & 0 \end{pmatrix} = \begin{pmatrix} 0 & -\omega \\ \omega & 0 \end{pmatrix}, \quad \text{with } \omega = \dot{\varphi}.$$

Each component of  $\mathbf{v}_X$  can be calculated explicitly as

$$\dot{x}_0 = \dot{d}_x - \omega(y_0 - d_y) \quad \text{and} \quad \dot{y}_0 = \dot{d}_y + \omega(x_0 - d_x).$$

### 2.3.2. Velocity distribution

The velocity distribution of a planar motion gives information about how the movement of any two points of the system is connected. By Theorem 1 any two positions of a system can be mapped onto each other by revolution or translation. For any planar motion it is possible to consider its instantaneous properties. Depending on the value of the angular velocity  $\omega$  and the translation vector  $\mathbf{d}$ , there are three possible cases:

1. **instantaneous revolution** ( $\omega \neq 0$ )

There exists exactly one point  $P$  with vanishing velocity. That point  $P$  can be calculated as

$$p_x = d_x - \frac{\dot{d}_y}{\omega} \quad \text{and} \quad p_y = d_y + \frac{\dot{d}_x}{\omega}$$

with respect to the chosen coordinate frame in  $\Sigma_0$ .  $P$  is called the *instantaneous center of revolution* (ICR). The velocity vectors behave as in the case of a continuous revolution about the ICR  $P$ , with angular velocity  $\omega = \dot{\varphi}$  (see Fig. 2.4).

## 2. Kinematical fundamentals

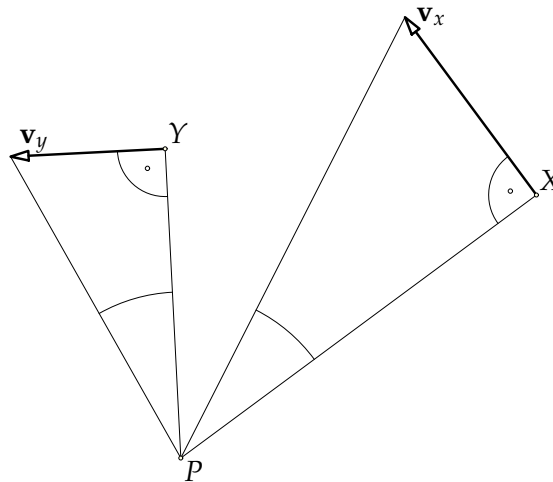


Figure 2.4.: Velocity distribution of an instantaneous revolution

### 2. instantaneous translation ( $\omega = 0$ and $\dot{\mathbf{d}} \neq 0$ )

Here we have  $\mathbf{W} = \begin{pmatrix} 0 & 0 \\ 0 & 0 \end{pmatrix}$  and from 2.4:

$$\mathbf{v}_x = \dot{\mathbf{d}}, \quad \forall X.$$

All points have the same velocity vector (see Fig. 2.5).

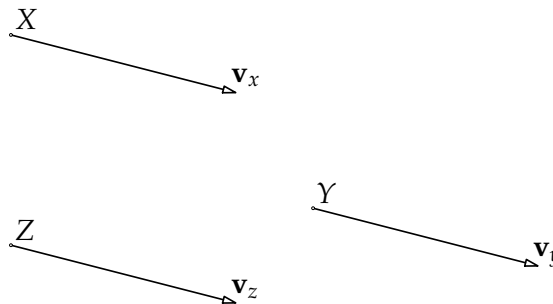


Figure 2.5.: Velocity distribution of an instantaneous translation

### 3. instantaneous standstill ( $\omega = 0$ and $\dot{\mathbf{d}} = 0$ )

All velocity vectors are vanishing.

## 2.4. Mechanisms

**Definition 3** (Mechanism).

1. A planar mechanism is built up from several rigid bodies also called systems  $\Sigma_0, \dots, \Sigma_{n-1}$  which are connected by joints.

## 2. Kinematical fundamentals

2. If for a particular mechanism, each of the  $\binom{n}{2}$  relative motions,  $\Sigma_j \setminus \Sigma_k$   $k, j = 0, \dots, n-1$ ;  $k < j$  of two of the rigid bodies is one parametric then we speak of a one parametric mechanism.
3. A mechanism, where each rigid body  $\Sigma_i$  is connected via joints with at least two of the other rigid bodies  $\Sigma_j, \Sigma_k$  is called a *closed mechanism*.

**Definition 4** (Revolute joint).

A *revolute joint* is a connection between two rigid bodies which allows only rotation about an axis  $a$ . (see Fig. 2.6)

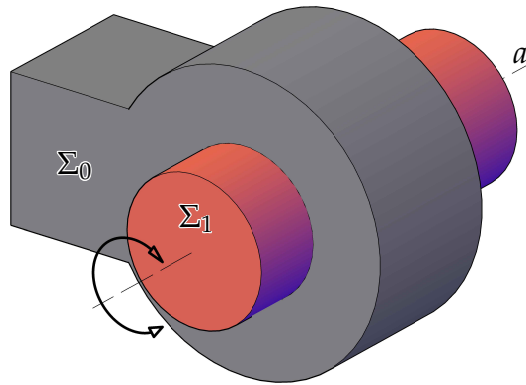


Figure 2.6.: Revolute joint

**Definition 5** (Theoretical degree of freedom). [2, p. 30-31]

Subsequently we study a planar mechanism with the systems  $\Sigma_0, \dots, \Sigma_{n-1}$  and  $m$  joints  $J_1, \dots, J_m$  connecting these systems. Let  $f_i$  denote the degree of freedom of the joint  $J_i$ ;  $f_i = 1, 2$ . We can think of  $\Sigma_0$  as being fixed whereas the remaining  $n-1$  systems  $\Sigma_1, \dots, \Sigma_{n-1}$  move with respect to  $\Sigma_0$ . At first imagine the mechanism without the joints. Each system then has three degrees of freedom with respect to the fixed system  $\Sigma_0$ . If every system  $\Sigma_i$ ,  $i = 0, \dots, n-1$  is equipped with a local coordinate frame  $\{O_i; \mathbf{e}_{i1}, \mathbf{e}_{i2}\}$ , the three degrees of freedom are the coordinates  $a_i, b_i$  of the origin  $O_i$  with respect to the fixed systems coordinate frame  $\{O_0; \mathbf{e}_{01}, \mathbf{e}_{02}\}$  and the angle  $\varphi_i := \angle(\mathbf{e}_{01}, \mathbf{e}_{i1})$ . This results in  $3 \cdot (n-1)$  parameters to describe all possible positions. By installing the joint  $J_i$ , the mechanism loses  $(3 - f_i)$  degrees of freedom. Hence, by mounting all joints we lose  $\sum_{i=1}^m (3 - f_i)$  degrees of freedom. Accordingly the theoretical degree of freedom (DOF) is defined as

$$f = 3 \cdot (n - 1) - \sum_{j=1}^m (3 - f_j). \quad (2.6)$$

MARTIN GRÜBLER found the formula for the *theoretical degree of freedom* in 1883: The formula of GRÜBLER only holds in the generic case, since it only

## 2. Kinematical fundamentals

counts conditions and parameters of a mechanism. The actual DOF can differ from the theoretical DOF.

A one parametric mechanism (see Def. 3.2) depends only on one input parameter. In this case each of the systems  $\Sigma_j$  of the mechanisms moves one parametrically with respect to any of the other systems  $\Sigma_i$ . By the concept of instantaneous movement, it is possible to construct the ICR  $P_{ij}$  of any of the  $\binom{n}{2}$  motions  $\Sigma_j \setminus \Sigma_i$ ,  $i, j = 0, \dots, n-1$ ,  $i < j$ .

**Theorem 2** (Threepole theorem of ARONHOLD-KENNEDY). [7, p. 120]

Let a one parametric planar mechanism be given and let  $\Sigma_0, \dots, \Sigma_{n-1}$  denote its systems. Let moreover  $P_{ij}$  be the ICR of the motion  $\Sigma_j \setminus \Sigma_i$  and  $\omega_{ij}$  be the instantaneous angular velocity of this motion at a chosen time instant  $t$ . Then the following holds for any three mutually distinct systems  $\Sigma_i, \Sigma_j, \Sigma_k$ :

The ICRs  $P_{ij}, P_{jk}, P_{ik}$  are collinear and moreover

$$\overrightarrow{P_{ij}P_{jk}} = \frac{\omega_{ik}}{\omega_{ij}} \cdot \overrightarrow{P_{ik}P_{jk}}. \quad (2.7)$$

- Remark 1.**
1. Equation 2.7 means that the ratio of the three collinear points  $P_{ij}, P_{jk}, P_{ik}$  is  $\frac{\omega_{ik}}{\omega_{ij}}$ .
  2. We call the line  $g_{ijk}$  containing the ICRs  $P_{ij}, P_{jk}, P_{ik}$  *pole axis*. Obviously, there exist  $\binom{n}{3} = \frac{n \cdot (n-1) \cdot (n-2)}{3 \cdot 2}$  pole axes for a one parametric planar mechanism with  $n$  systems at any time instant  $t$ . The geometrical configuration established by the  $\binom{n}{2}$  ICRs  $P_{ij}$  and the  $\binom{n}{3}$  pole axis  $g_{ijk}$  at a time instant  $t$  is called *ICR configuration*.

## 2.5. Example four bar linkage

### ICR configuration of a four bar linkage

In [7, p. 119 - 121], a *planar four bar linkage* is defined by an arbitrary planar quadrilateral ABCD (see Fig. 2.7): It consists of four systems  $\Sigma_0, \dots, \Sigma_3$  and four revolute joints  $J_0, \dots, J_3$ . The systems  $\Sigma_0, \dots, \Sigma_3$  are represented by the quadrilaterals edges  $AB, AD, BC, CD$  and the revolute joints  $J_0, \dots, J_3$  are centered in the quadrilaterals vertices  $A, B, C, D$ . The system  $\Sigma_0$  is called the (fixed) base of the mechanism. The arm  $\Sigma_1$  of the mechanism gets driven, which is called crank or rocker, depending on whether a full revolution

## 2. Kinematical fundamentals

of this arm is possible. The second arm  $\Sigma_2$  can also have the function of a crank or a rocker and the fourth bar is called the coupler  $\Sigma_3$ . To check, if the motion of a four bar linkage is one parametric, we will calculate the theoretical DOF as in 2.6. A four bar linkage has  $n = 4$  systems and for a revolute joint  $f_i = 1$ . The theoretical DOF results in

$$f = 3 \cdot (4 - 1) - \sum_{j=1}^4 (3 - 1) = 1.$$

Since  $n = 4$ , there are  $\binom{4}{2} = 6$  ICRs and  $\binom{4}{3} = 4$  pole axes. Clearly, four of the ICRs are the points  $A, B, C, D$ :  $P_{01} = A$ ,  $P_{02} = B$ ,  $P_{23} = C$  and  $P_{13} = D$ . With these four ICRs the pole axes can be constructed:  $g_{012} = AB$ ,  $g_{013} = AD$ ,  $g_{023} = BC$  and  $g_{123} = CD$ . With Theorem 2 the two remaining poles  $P_{03}$  and  $P_{12}$  can be constructed as  $P_{03} = g_{013} \cap g_{023}$  and  $P_{12} = g_{012} \cap g_{123}$  (see Fig. 2.7).

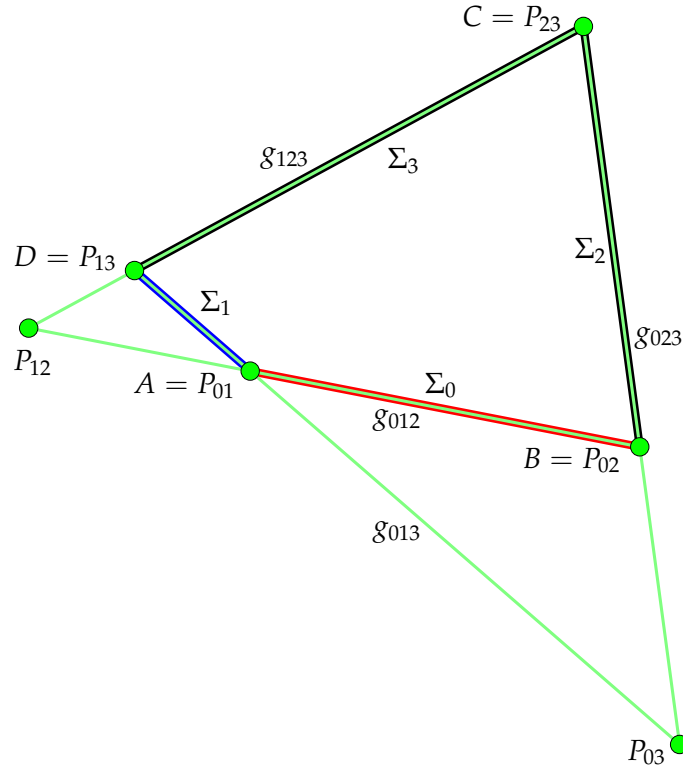


Figure 2.7.: ICR configuration of a four bar linkage

### Geometrical analysis of the velocities of a four bar linkage

According to [7, p. 23], when the crank  $AD$  of the four bar linkage is driven with a particular instantaneous angular velocity  $\omega_{01}$  at the time instant  $t$ ,

## 2. Kinematical fundamentals

then we also know the velocity vector  $\mathbf{v}_{D,01}$  of the point  $D$  with respect to the motion  $\Sigma_1 \setminus \Sigma_0$  (see Fig. 2.8). With  $\mathbf{v}_{D,01}$  given, it is easy to determine the velocity vector  $\mathbf{v}_{C,ij}$  of any point  $X \in \Sigma_j$  with respect to the motion  $\Sigma_j \setminus \Sigma_i$ . Choose for instance,  $i = 0, j = 2$  and hence  $C \in \Sigma_2$ , then the construction of  $\mathbf{v}_{C,02}$  can be done as follows:

The velocity  $\mathbf{v}_{D,13}$  is zero, as  $D$  is the pole  $P_{13}$ . Since velocities are additive, we can calculate

$$\mathbf{v}_{D,01} + \underbrace{\mathbf{v}_{D,13}}_{=0} = \mathbf{v}_{D,03} \Rightarrow \mathbf{v}_{D,01} = \mathbf{v}_{D,03}.$$

We use the velocity  $\mathbf{v}_{D,03}$  to construct the velocity  $\mathbf{v}_{C,03}$ . To achieve this, we have to rotate the vector  $\mathbf{v}_{D,03}$  by  $90^\circ$  around  $D$  to get a point  $X$  on the line  $AD$ . We construct a parallel line to  $CD$  through the point  $X$  to get a point  $Y$  where the parallel intersects  $BC$ . By rotating  $Y$  around  $C$  by  $90^\circ$  in the reverse direction of the previous rotation, we get the vector  $\mathbf{v}_{C,03}$  of the velocity of the point  $C$  with respect to the pole  $P_{03}$ . By knowing  $\mathbf{v}_{C,03}$ , we can calculate

$$\mathbf{v}_{C,02} + \underbrace{\mathbf{v}_{C,23}}_{=0} = \mathbf{v}_{C,03} \Rightarrow \mathbf{v}_{C,02} = \mathbf{v}_{C,03}.$$

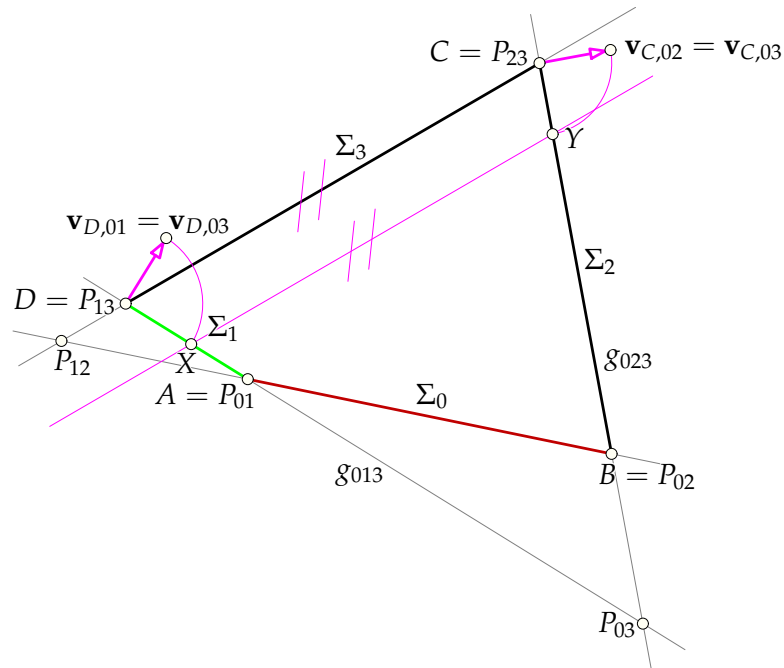


Figure 2.8.: Velocity distribution of a four bar linkage

## 2. Kinematical fundamentals

### Analysis of a four bar linkage

In order to get a parametrization of a four bar linkage, it is necessary to know the dependencies of the angles. With respect to the *drive angle*  $\varphi_1 = t$ , the *output angle*  $\varphi_2(t)$  of the second arm and the *angle of the coupler*  $\varphi_3(t)$  can be calculated (see Fig. 2.9).

The bar  $AB$  with length  $d$  is fixed and let  $BC$  and  $AD$  be the arms of such a linkage. The driving arm  $AD$  has length  $a$  and the second arm has length  $b$ . The length of the coupler  $CD$  is  $c$ . We use a right coordinate frame  $F = \{O, \mathbf{e}_x, \mathbf{e}_y\}$  with  $O = A$  and  $\mathbf{e}_x = \frac{\vec{AB}}{\|AB\|}$ .

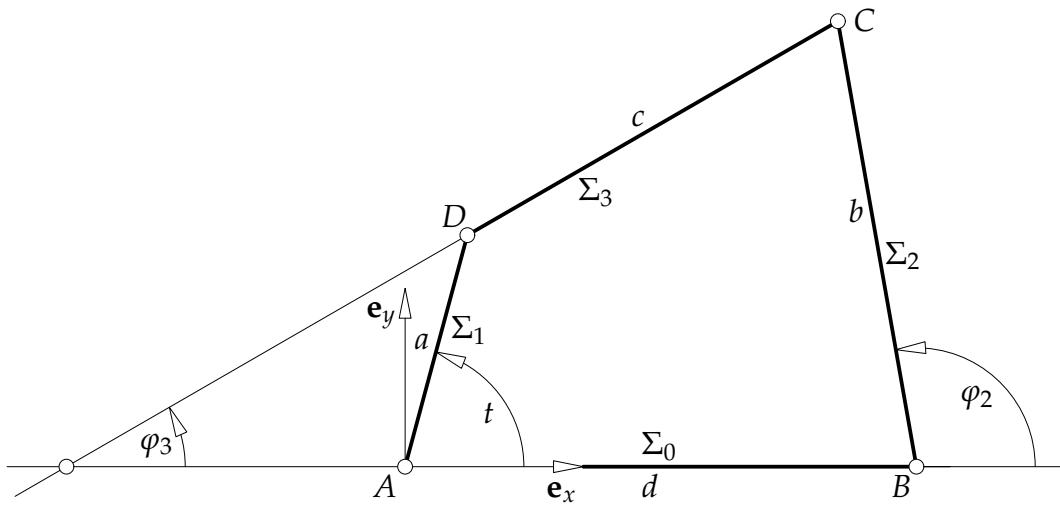


Figure 2.9.: Notations of a four bar linkage

## 2. Kinematical fundamentals

### Dependencies of the angles of a four bar linkage – calculations

The coordinates of the points  $A, B, C, D$  with respect to the coordinate frame in  $\Sigma_0$  can be calculated with elementary trigonometry for the dimensions shown in Figure 2.9.

$$A : \begin{pmatrix} x_A \\ y_A \end{pmatrix} = \begin{pmatrix} 0 \\ 0 \end{pmatrix} \quad (2.8)$$

$$B : \begin{pmatrix} x_B \\ y_B \end{pmatrix} = \begin{pmatrix} d \\ 0 \end{pmatrix} \quad (2.9)$$

$$D : \begin{pmatrix} x_D \\ y_D \end{pmatrix} = \begin{pmatrix} a \cos(t) \\ a \sin(t) \end{pmatrix} \quad (2.10)$$

$$C : \begin{pmatrix} x_C \\ y_C \end{pmatrix} = \begin{pmatrix} x_D + c \cos(\varphi_3) = x_B + b \cos(\varphi_2) \\ y_D + c \sin(\varphi_3) = y_B + b \sin(\varphi_2) \end{pmatrix} \quad (2.11)$$

By substituting 2.9 and 2.10 in the right side of 2.11, we obtain the following two equations :

$$a \cdot \cos(t) - b \cdot \cos(\varphi_2) + c \cdot \cos(\varphi_3) = d. \quad (2.12)$$

$$a \cdot \sin(t) - b \cdot \sin(\varphi_2) + c \cdot \sin(\varphi_3) = 0. \quad (2.13)$$

$\varphi_3$  can be eliminated by isolating all parts with  $\varphi_3$  on the right hand side to square and add the equations 2.12 and 2.13:

$$a \cdot \cos(t) - b \cdot \cos(\varphi_2) - d = -c \cdot \cos(\varphi_3) \quad (2.14)$$

$$a \cdot \sin(t) - b \cdot \sin(\varphi_2) = -c \cdot \sin(\varphi_3). \quad (2.15)$$

$$\begin{aligned} a^2 + b^2 + d^2 - 2ab \cdot (\cos(t) \cos(\varphi_2) + \sin(t) \sin(\varphi_2)) \\ - 2d \cdot (a \cdot \cos(t) - b \cos(\varphi_2)) - c^2 = 0 \end{aligned} \quad (2.16)$$

As an interim result, the equation for  $\varphi_2$  can be written as:

$$A_2 \cdot \cos(\varphi_2) + B_2 \cdot \sin(\varphi_2) + C_2 = 0 \quad (2.17)$$

with:

$$\begin{aligned} A_2 &:= 2b(d - a \cos(t)) \\ B_2 &:= -2ab \sin(t) \\ C_2 &:= a^2 + b^2 - c^2 + d^2 - 2ad \cos(t) \end{aligned} \quad (2.18)$$

To calculate  $\varphi_2$ , the property  $\sin(\varphi_2) = \pm \sqrt{1 - \cos^2(\varphi_2)}$  of the trigonometric functions is used in 2.17, which is squared to get rid of the root.

$$\begin{aligned} A_2 \cdot \cos(\varphi_2) + C_2 &= \mp B_2 \cdot \sqrt{1 - \cos^2(\varphi_2)} \\ (A_2^2 + B_2^2) \cos^2 \varphi_2 + 2A_2 C_2 \cos(\varphi_2) - B_2^2 + C_2^2 &= 0 \end{aligned}$$

## 2. Kinematical fundamentals

Hence, we obtain:

$$\begin{aligned}
 \cos(\varphi_2) &= \frac{-2A_2C_2 \pm \sqrt{4A_2^2C_2^2 - 4(A_2^2 + B_2^2)(-B_2^2 + C_2^2)}}{2(A_2^2 + B_2^2)} \\
 &= \frac{-A_2C_2 \pm \sqrt{A_2^2C_2^2 - A_2^2C_2^2 + A_2^2B_2^2 + B_2^4 - B_2^2C_2^2}}{A_2^2 + B_2^2} \\
 &= \frac{-A_2C_2 \pm B_2 \cdot \sqrt{A_2^2 + B_2^2 - C_2^2}}{A_2^2 + B_2^2}.
 \end{aligned}$$

With 2.17 also the sine of  $\varphi_2$  can be calculated:

$$\begin{aligned}
 \sin(\varphi_2) &= \frac{-A_2 \cdot \cos(\varphi_2) - C_2}{B_2} \\
 &= \frac{A_2C_2 \mp A_2B_2 \cdot \sqrt{A_2^2 + B_2^2 - C_2^2} - C_2 \cdot (A_2^2 + B_2^2)}{B_2 \cdot (A_2^2 + B_2^2)} \\
 &= \frac{-B_2C_2 \mp A_2 \cdot \sqrt{A_2^2 + B_2^2 - C_2^2}}{A_2^2 + B_2^2}.
 \end{aligned}$$

Similar calculations are necessary to get the angle  $\varphi_3$  as a function of  $t$ . This means that we have to eliminate  $\varphi_2$  from the equations 2.12 and 2.13. By collecting the terms without  $\varphi_2$  on the left hand side we get

$$a \cdot \cos(t) + c \cdot \cos(\varphi_3) - d = b \cdot \cos(\varphi_2) \quad (2.19)$$

$$a \cdot \sin(t) + c \cdot \sin(\varphi_3) = b \cdot \sin(\varphi_2). \quad (2.20)$$

Squaring and adding yields to

$$A_3 \cdot \cos(\varphi_3) + B_3 \cdot \sin(\varphi_3) + C_3 = 0 \quad (2.21)$$

with

$$\begin{aligned}
 A_3 &:= 2c(a \cos(t) - d) \\
 B_3 &:= 2ac \sin(t) \\
 C_3 &:= a^2 - b^2 + c^2 + d^2 - 2ad \cos(t)
 \end{aligned} \quad (2.22)$$

By comparing 2.17 with 2.21 it is easy to see that it is the same equation, except the first one is in the parameter  $\varphi_2$  and the second one in the parameter  $\varphi_3$ . Therefore the result of 2.17 can also be used for  $\varphi_3$ .

## 2. Kinematical fundamentals

### Dependencies of the angles of a four bar linkage – result

The sine and cosine of the angles  $\varphi_2$  and  $\varphi_3$  can be calculated with the same formula and different coefficients  $A_i, B_i, C_i$  for  $i = 2, 3$  as follows:

$$\cos \varphi_i = \frac{-A_i C_i \pm B_i \cdot \sqrt{A_i^2 + B_i^2 - C_i^2}}{A_i^2 + B_i^2} \quad (2.23)$$

$$\sin \varphi_i = \frac{-B_i C_i \mp A_i \cdot \sqrt{A_i^2 + B_i^2 - C_i^2}}{A_i^2 + B_i^2}. \quad (2.24)$$

For the angle  $\varphi_2$  the parameters are

$$\begin{aligned} A_2 &= 2b(d - a \cos(t)) \\ B_2 &= -2ab \sin(t) \\ C_2 &= a^2 + b^2 - c^2 + d^2 - 2ad \cos(t) \end{aligned} \quad (2.25)$$

and for the angle  $\varphi_3$  the parameters are

$$\begin{aligned} A_3 &= 2c(a \cos(t) - d) \\ B_3 &= 2ac \sin(t) \\ C_3 &= a^2 - b^2 + c^2 + d^2 - 2ad \cos(t) \end{aligned} \quad (2.26)$$

A four bar linkage can be assembled in two different ways (a) and (b) with the same drive angle, and therefore the Equations 2.23 – 2.24 have an ambiguity in terms of the used signs. One can easily check that the following combinations are the correct ones for the two assembly modes:

$$\begin{aligned} \text{(a)} \quad \cos \varphi_2 &= \frac{-A_2 C_2 + B_2 \cdot \sqrt{A_2^2 + B_2^2 - C_2^2}}{A_2^2 + B_2^2}, & \sin \varphi_2 &= \frac{-B_2 C_2 - A_2 \cdot \sqrt{A_2^2 + B_2^2 - C_2^2}}{A_2^2 + B_2^2} \\ \cos \varphi_3 &= \frac{-A_3 C_3 - B_3 \cdot \sqrt{A_3^2 + B_3^2 - C_3^2}}{A_3^2 + B_3^2}, & \sin \varphi_3 &= \frac{-B_3 C_3 + A_3 \cdot \sqrt{A_3^2 + B_3^2 - C_3^2}}{A_3^2 + B_3^2} \\ \text{(b)} \quad \cos \varphi_2 &= \frac{-A_2 C_2 - B_2 \cdot \sqrt{A_2^2 + B_2^2 - C_2^2}}{A_2^2 + B_2^2}, & \sin \varphi_2 &= \frac{-B_2 C_2 + A_2 \cdot \sqrt{A_2^2 + B_2^2 - C_2^2}}{A_2^2 + B_2^2} \\ \cos \varphi_3 &= \frac{-A_3 C_3 + B_3 \cdot \sqrt{A_3^2 + B_3^2 - C_3^2}}{A_3^2 + B_3^2}, & \sin \varphi_3 &= \frac{-B_3 C_3 - A_3 \cdot \sqrt{A_3^2 + B_3^2 - C_3^2}}{A_3^2 + B_3^2} \end{aligned}$$

## 2. Kinematical fundamentals

### Parametrization of a four bar linkage

We choose local coordinate frames  $\{O_i; \mathbf{e}_{i1}, \mathbf{e}_{i2}\}$  in the systems  $\Sigma_i; i = 0, 1, 2, 3$  as follows (see Fig. 2.10):

$$O_0 = A; \quad \mathbf{e}_{01} = \frac{\overrightarrow{AB}}{\|AB\|} \quad (2.27)$$

$$O_1 = A; \quad \mathbf{e}_{11} = \frac{\overrightarrow{AD}}{\|AD\|} \quad (2.28)$$

$$O_2 = B; \quad \mathbf{e}_{21} = \frac{\overrightarrow{BC}}{\|BC\|} \quad (2.29)$$

$$O_3 = D; \quad \mathbf{e}_{31} = \frac{\overrightarrow{DC}}{\|DC\|} \quad (2.30)$$

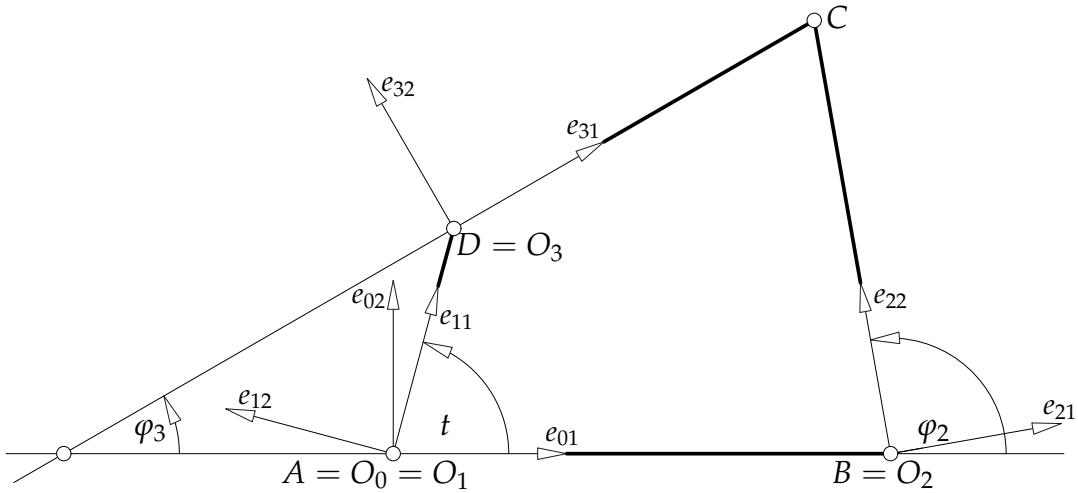


Figure 2.10.: Coordinate frames used for the parametrization of a four bar linkage

With respect to these coordinate frames the motions  $\Sigma_1 \setminus \Sigma_0$ ,  $\Sigma_2 \setminus \Sigma_0$  and  $\Sigma_3 \setminus \Sigma_0$  are parametrized as follows:

$$\Sigma_1 \setminus \Sigma_0 : \begin{pmatrix} 1 \\ x_0 \\ y_0 \end{pmatrix} = \begin{pmatrix} 1 & 0 & 0 \\ 0 & \cos(t) & -\sin(t) \\ 0 & \sin(t) & \cos(t) \end{pmatrix} \begin{pmatrix} 1 \\ x_1 \\ y_1 \end{pmatrix} \quad (2.31)$$

## 2. Kinematical fundamentals

$$\Sigma_2 \setminus \Sigma_0 : \begin{pmatrix} 1 \\ x_0 \\ y_0 \end{pmatrix} = \begin{pmatrix} 1 & 0 & 0 \\ d & \cos(\varphi_2(t)) & -\sin(\varphi_2(t)) \\ 0 & \sin(\varphi_2(t)) & \cos(\varphi_2(t)) \end{pmatrix} \begin{pmatrix} 1 \\ x_2 \\ y_2 \end{pmatrix} \quad (2.32)$$

$$\Sigma_3 \setminus \Sigma_0 : \begin{pmatrix} 1 \\ x_0 \\ y_0 \end{pmatrix} = \begin{pmatrix} 1 & 0 & 0 \\ a \cdot \cos(t) & \cos(\varphi_3(t)) & -\sin(\varphi_3(t)) \\ a \cdot \sin(t) & \sin(\varphi_3(t)) & \cos(\varphi_3(t)) \end{pmatrix} \begin{pmatrix} 1 \\ x_3 \\ y_3 \end{pmatrix} \quad (2.33)$$

By means of [2.31](#), [2.32](#) and [2.33](#) the position of any point in  $\Sigma_1, \Sigma_2$  and  $\Sigma_3$  with respect to  $\Sigma_0$  can be computed in dependency of the motion parameter  $t$  (= drive angle).

## 3. Analysis of the Jansen mechanism

### 3.1. Description of the Jansen mechanism

Theo Jansen's leg mechanism is illustrated in Fig. 3.1. It consists of  $n = 8$  systems  $\Sigma_0, \dots, \Sigma_7$  and  $m = 10$  revolute joints. We use a different notation to that of Theo Jansen for his holy numbers, so Table 3.1 gives a comparison of the distinct notations.

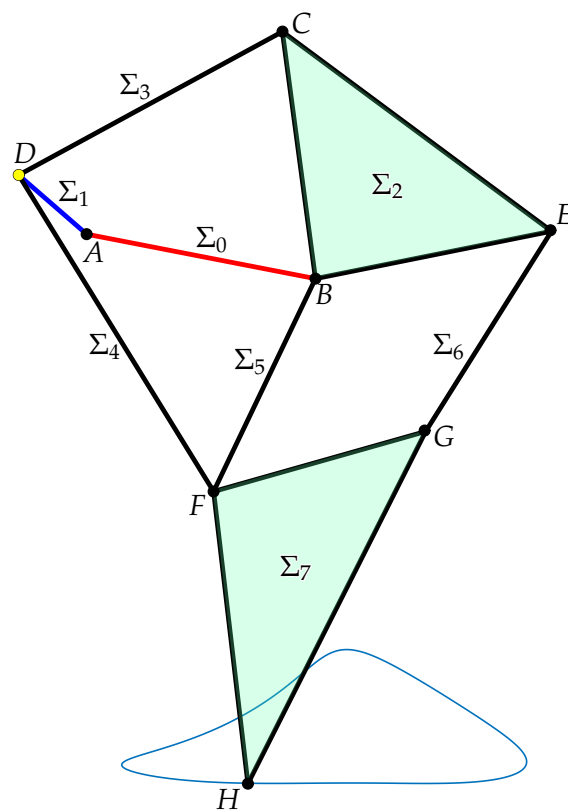


Figure 3.1.: Notation of the systems for the ICR configuration of the Jansen mechanism

The systems  $\Sigma_0, \Sigma_1, \Sigma_3, \Sigma_4, \Sigma_5$  and  $\Sigma_6$  are visualized as bars  $AB, AD, CD, DF, BF$  and  $EG$  whereas the remaining two systems  $\Sigma_2$  and  $\Sigma_7$  are represented

### 3. Analysis of the Jansen mechanism

Holy numbers	systems	new notations
$a^* = 38.0$	-	$d_{1,x}$
$b^* = 41.5$	$\Sigma_2$	$b_1$
$c^* = 39.3$	$\Sigma_5$	$b_2 = a_3$
$d^* = 40.1$	$\Sigma_2$	$d_3$
$e^* = 55.8$	$\Sigma_2$	$e$
$f^* = 39.4$	$\Sigma_6$	$b_3$
$g^* = 36.7$	$\Sigma_7$	$c_3$
$h^* = 65.7$	$\Sigma_7$	$f$
$i^* = 49.0$	$\Sigma_7$	$g$
$j^* = 50.0$	$\Sigma_3$	$c_1$
$k^* = 61.9$	$\Sigma_4$	$c_2$
$l^* = 7.8$	-	$d_{1,y}$
$m^* = 15.0$	$\Sigma_1$	$a_1 = a_2$
$n^* = \sqrt{a^{*2} + l^{*2}} \approx 38.8$	$\Sigma_0$	$d_1 = d_2$

Table 3.1.: Notations of the Jansen mechanism and our notations

by the triangles  $BCE$  and  $FGH$ , respectively. The table 3.2 depicts which systems are connected by the ten revolute joints.

So each of the points  $B, D$  and  $F$  is center of two revolute joints, whereas in  $A, C, D, E$  and  $G$  only one revolute joint is centered.

By means of GRÜBLER's formula we obtain a theoretical DOF of

$$f = 3 \cdot (n - 1) - \sum_{i=1}^m (3 - f_i) = 3 \cdot 7 - \sum_{i=1}^{10} 2 = 1$$

#	system	system	connected by revolute joint centered in
1	$\Sigma_0$	$\Sigma_1$	A
2	$\Sigma_0$	$\Sigma_2$	B
3	$\Sigma_0$	$\Sigma_5$	B
4	$\Sigma_2$	$\Sigma_3$	C
5	$\Sigma_1$	$\Sigma_3$	D
6	$\Sigma_1$	$\Sigma_4$	D
7	$\Sigma_2$	$\Sigma_6$	E
8	$\Sigma_4$	$\Sigma_5$	F
9	$\Sigma_4$	$\Sigma_7$	F
10	$\Sigma_6$	$\Sigma_7$	G

Table 3.2.: List of revolute joints and the connected bars of the Jansen mechanism

### 3. Analysis of the Jansen mechanism

Second four bar linkage ( $\Sigma_0, \Sigma_1, \Sigma_5, \Sigma_4$ )			
$P_{01} = A$	$P_{05} = B$	$P_{14} = D$	$P_{45} = F$
$g_{015} = AB$	$g_{014} = AD$	$g_{045} = BF$	$g_{145} = DF$
$P_{04} = g_{014} \cap g_{045}$		$P_{15} = g_{015} \cap g_{145}$	
see Fig. 3.2			

Table 3.3.: Construction protocol of the second four bar linkage of the Jansen mechanism.

of Jansen's mechanism. Subsequently we think of  $\Sigma_0$  as the *fixed system* (base) and call  $\Sigma_7$  *end effector*. The main focus will lie on the path of the foot tip  $H$  with respect to the motion  $\Sigma_7 \setminus \Sigma_0$  (end effector \ base). The flat part of this path corresponds to the ground contact of the leg.

## 3.2. ICR configuration of the Jansen mechanism

The example of the ICR configuration of a four bar linkage in 2.5, was constructed with the dimensions of the Jansen mechanism to serve as the basis for further constructions. The construction for this first four bar linkage ( $\Sigma_0, \Sigma_1, \Sigma_2, \Sigma_3$ ) is documented in Figure 2.7. We will add the next systems in small groups to complete new four bar linkages, in order to make it easy to follow the construction. The systems notations can be seen in Figure 3.1.

By adding  $\Sigma_4$  and  $\Sigma_5$  we obtain two additional four bar linkages, namely ( $\Sigma_0, \Sigma_1, \Sigma_5, \Sigma_4$ ) and ( $\Sigma_3, \Sigma_4, \Sigma_2, \Sigma_5$ ). By adding these two systems the number of poles increases to 15 and there will be 20 pole axes. We will use the previous construction for the ICR configuration for four bar linkages again and by doing so it is possible to find all the poles of the entire mechanism. The pole axes are constructed as in Theorem 2.

We will start with the four bar linkage ( $\Sigma_0, \Sigma_1, \Sigma_5, \Sigma_4$ ). The pole  $P_{01}$  is already known, so there will be only five new poles. The poles and pole axes which belong to each four bar linkage are in green shade and the previously constructed poles are in red shade (see Fig. 3.2 and Table 3.3).

With the given systems, it is possible to identify the systems ( $\Sigma_3, \Sigma_4, \Sigma_2, \Sigma_5$ ) as a four bar linkage. When constructing the ICR configuration of that four bar linkage, only four poles will be new, the rest are already existing poles. With these poles we have found all the poles of the mechanism so far (see Fig. 3.3 and Table 3.4).

### 3. Analysis of the Jansen mechanism

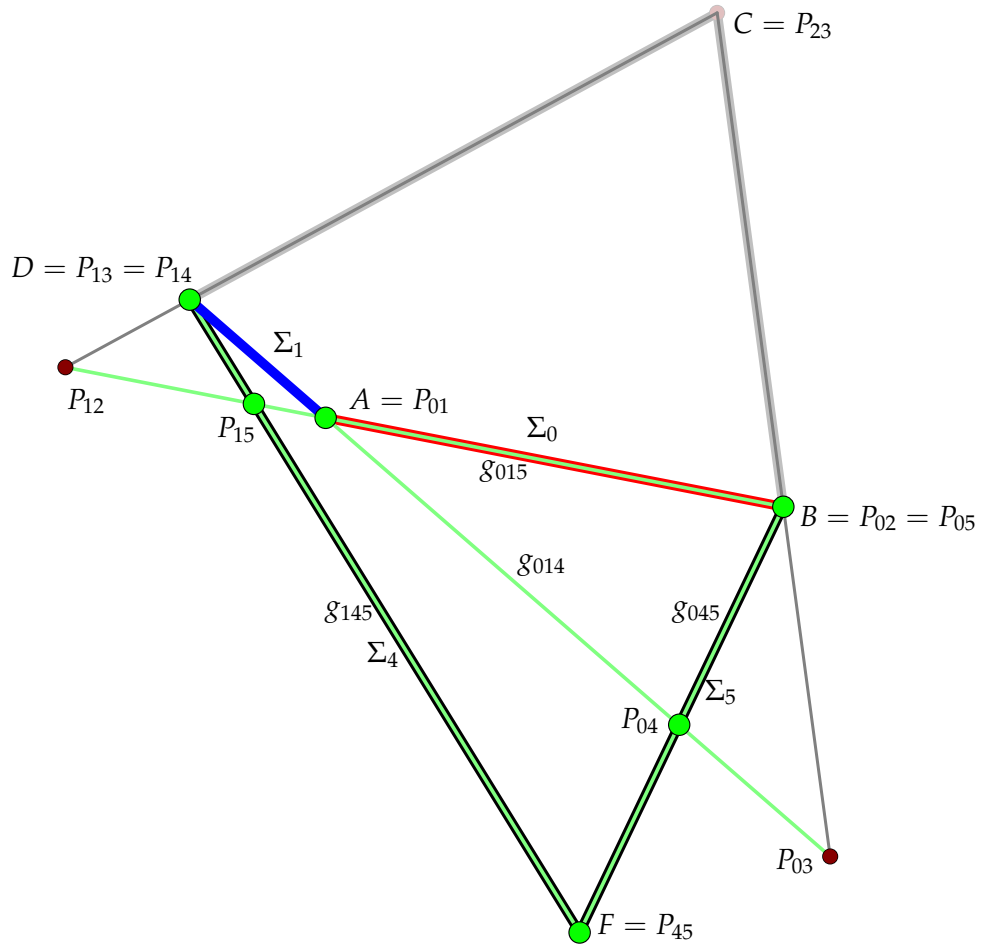


Figure 3.2.: ICR configuration of the second four bar linkage

Third four bar linkage ( $\Sigma_3, \Sigma_4, \Sigma_2, \Sigma_5$ )			
$P_{34} = D$	$P_{45} = F$	$P_{23} = C$	$P_{25} = B$
$g_{234} = CD$	$g_{235} = BC$	$g_{245} = BF$	$g_{345} = CD$
$P_{24} = g_{234} \cap g_{245}$		$P_{35} = g_{035} \cap g_{345}$	
see Fig. 3.3			

Table 3.4.: Construction protocol of the third bar linkage of the Jansen mechanism.

### 3. Analysis of the Jansen mechanism

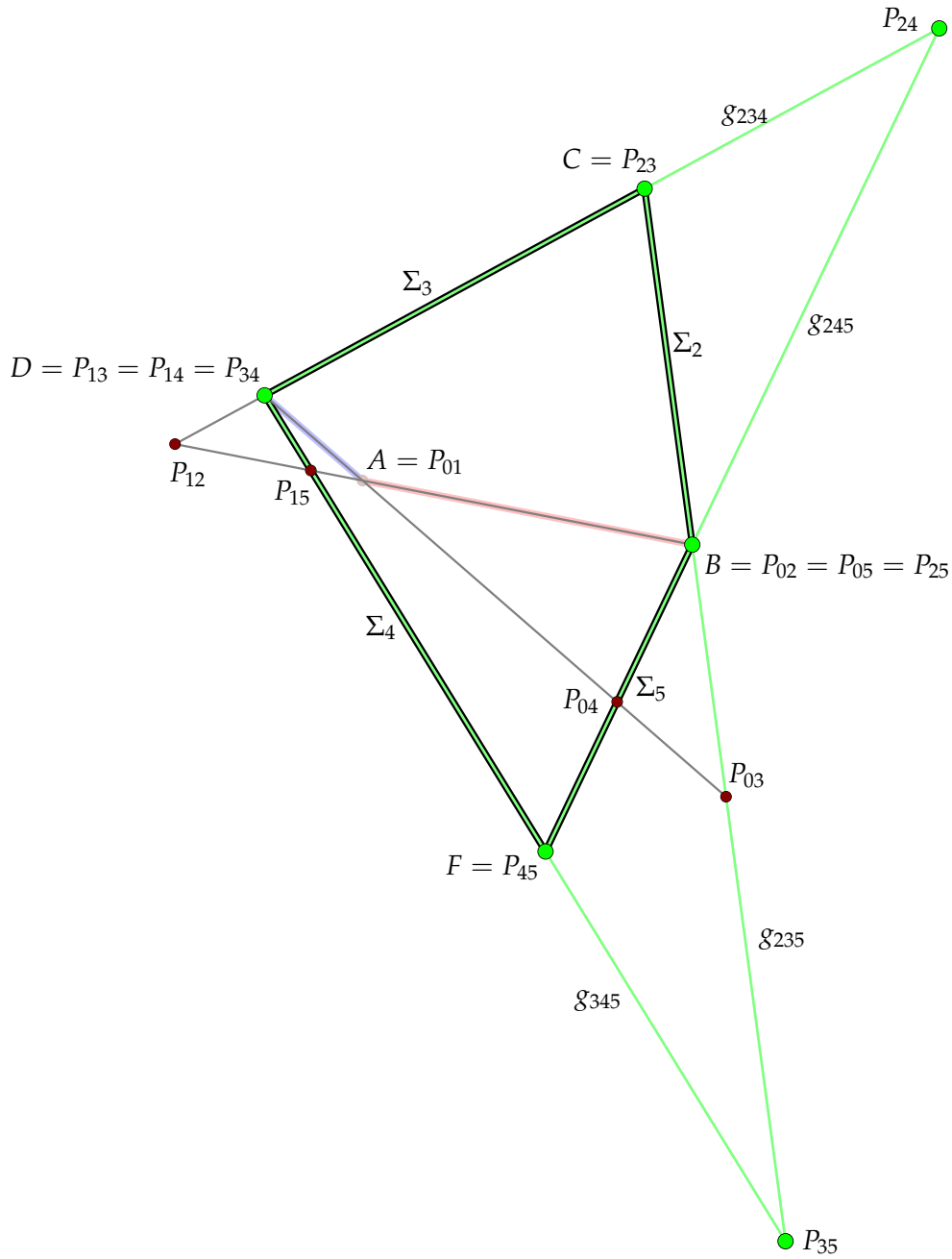


Figure 3.3.: ICR configuration of the third four bar linkage

### 3. Analysis of the Jansen mechanism

The points  $B$  and  $D$  were poles in each of the previous four bar linkages, which means  $B = P_{02} = P_{05} = P_{25}$  and  $D = P_{13} = P_{14} = P_{34}$ . Looking at the point  $B$  the pole axis  $g_{025}$ , which connects the three poles, collapses in the point  $B$  and the pole axis  $g_{134}$  collapses into the point  $D$ . The six other missing pole axes can be constructed as follows:  $g_{035} = g_{023}$ ,  $g_{124} = g_{123}$ ,  $g_{125} = g_{012}$ ,  $g_{034} = g_{013}$ ,  $g_{024} = g_{045}$  and  $g_{135} = g_{145}$ .

The fourth four bar linkage consists of the systems  $(\Sigma_2, \Sigma_5, \Sigma_6, \Sigma_7)$ , so the systems  $\Sigma_6$  and  $\Sigma_7$  are added to the mechanism. Again, we start by looking at the four bar linkage itself (see Fig. 3.4 and Table 3.5) and then construct the poles with respect to the other systems.

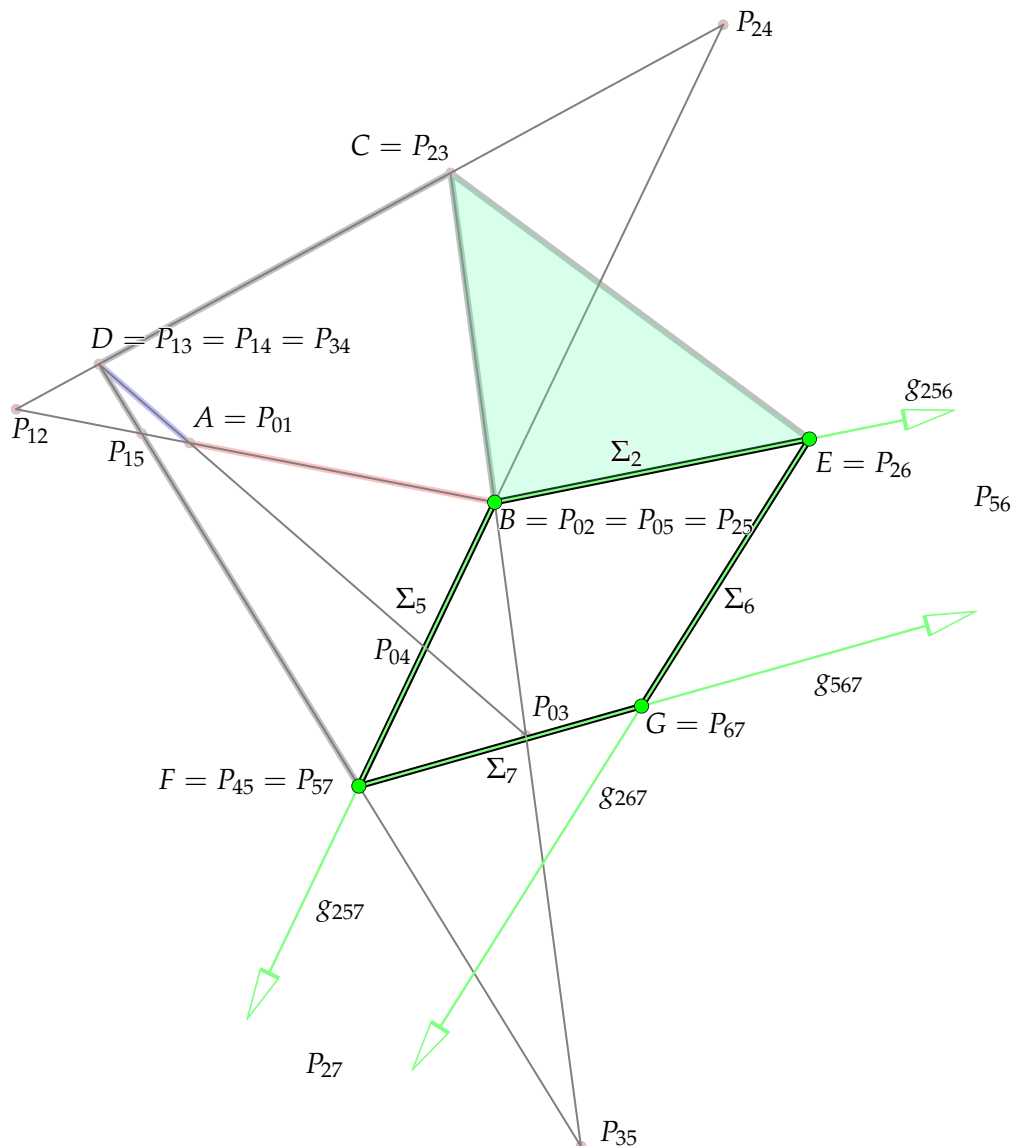


Figure 3.4.: ICR configuration of the fourth four bar linkages used in the Jansen mechanism

### 3. Analysis of the Jansen mechanism

Fourth four bar linkage ( $\Sigma_2, \Sigma_5, \Sigma_6, \Sigma_7$ )			
$P_{25} = B$	$P_{26} = E$	$P_{57} = F$	$P_{67} = G$
$g_{256} = BE$	$g_{257} = BF$	$g_{267} = EG$	$g_{567} = FG$
$P_{27} = g_{257} \cap g_{267}$		$P_{56} = g_{256} \cap g_{567}$	
see Fig. 3.4			

Table 3.5.: Construction protocol of the fourth four bar linkages of the Jansen mechanism.

Until now, we have found 20 poles and 24 pole axes. In order to get the rest of the poles, Theorem 2 has to be applied several times. The order of finding new poles can vary, but the final result is unique.

The foot tip  $H \in \Sigma_7$  is of special interest, therefore we are especially looking for the pole  $P_{07}$ . A short way to construct the pole  $P_{07}$  is by constructing the pole axes  $g_{127} = P_{12} \cup P_{27}$  and  $g_{157} = g_{135}$ . The intersection of these two pole axes yields the pole  $P_{17} = g_{127} \cap g_{157}$ . Now we can construct the pole axes  $g_{027} = g_{024}$  and  $g_{017} = A \cup P_{17}$  and get the pole  $P_{07}$  by intersecting these pole axes:  $P_{07} = g_{017} \cap g_{027}$  (see Fig. 3.5). The interested reader can confirm this and also construct the remaining poles and pole axes as no detailed protocol of the construction is delivered in this thesis.

By Subsection 2.3.2, the instantaneous movement of any point can be seen as a revolution regarding its pole. In order to construct the tangential direction for the movement of  $H$ , the pole  $P_{07}$  is connected with  $H$  and to get the tangent the line through  $H$  perpendicular to  $P_{07}H$  is constructed.

The finished ICR configuration of the Jansen mechanism consists of 28 poles and 56 pole axes and can be seen in Figure 3.6.

### 3.3. Geometrical analysis of the velocities of the Jansen mechanism

We use the methods of constructing the velocities of the joints of the Jansen mechanism as shown in Fig. 2.8. The dimensions of the four bar linkage are identical to the top part of the Jansen mechanism, so the previous result serves as a basis for further constructions. We already know that  $\mathbf{v}_{D,01} = \mathbf{v}_{D,03}$  and with the same argument we get  $\mathbf{v}_{D,01} = \mathbf{v}_{D,04}$ .

### 3. Analysis of the Jansen mechanism

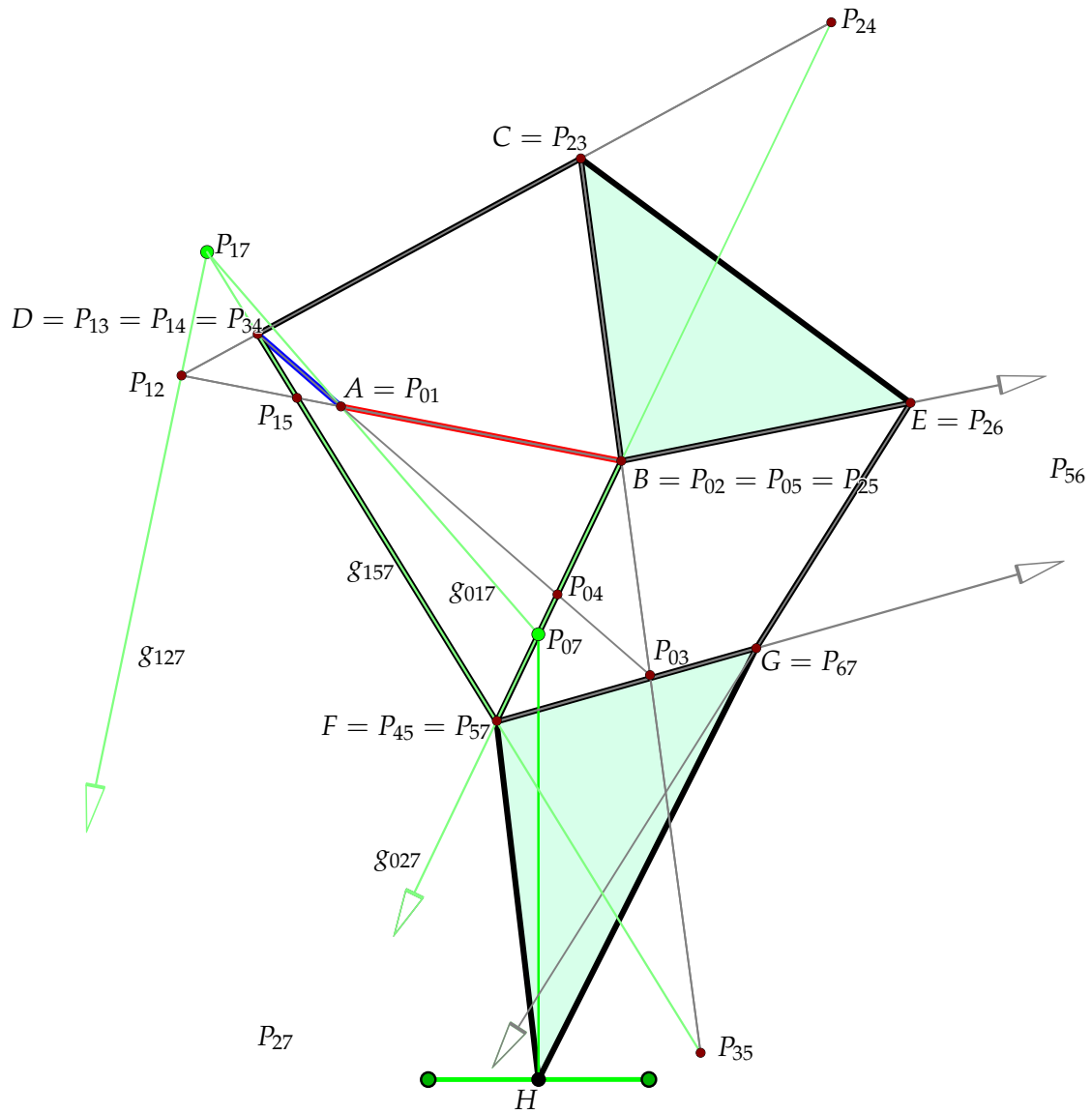


Figure 3.5.: ICR configuration: Construction of pole  $P_{07}$

### 3. Analysis of the Jansen mechanism

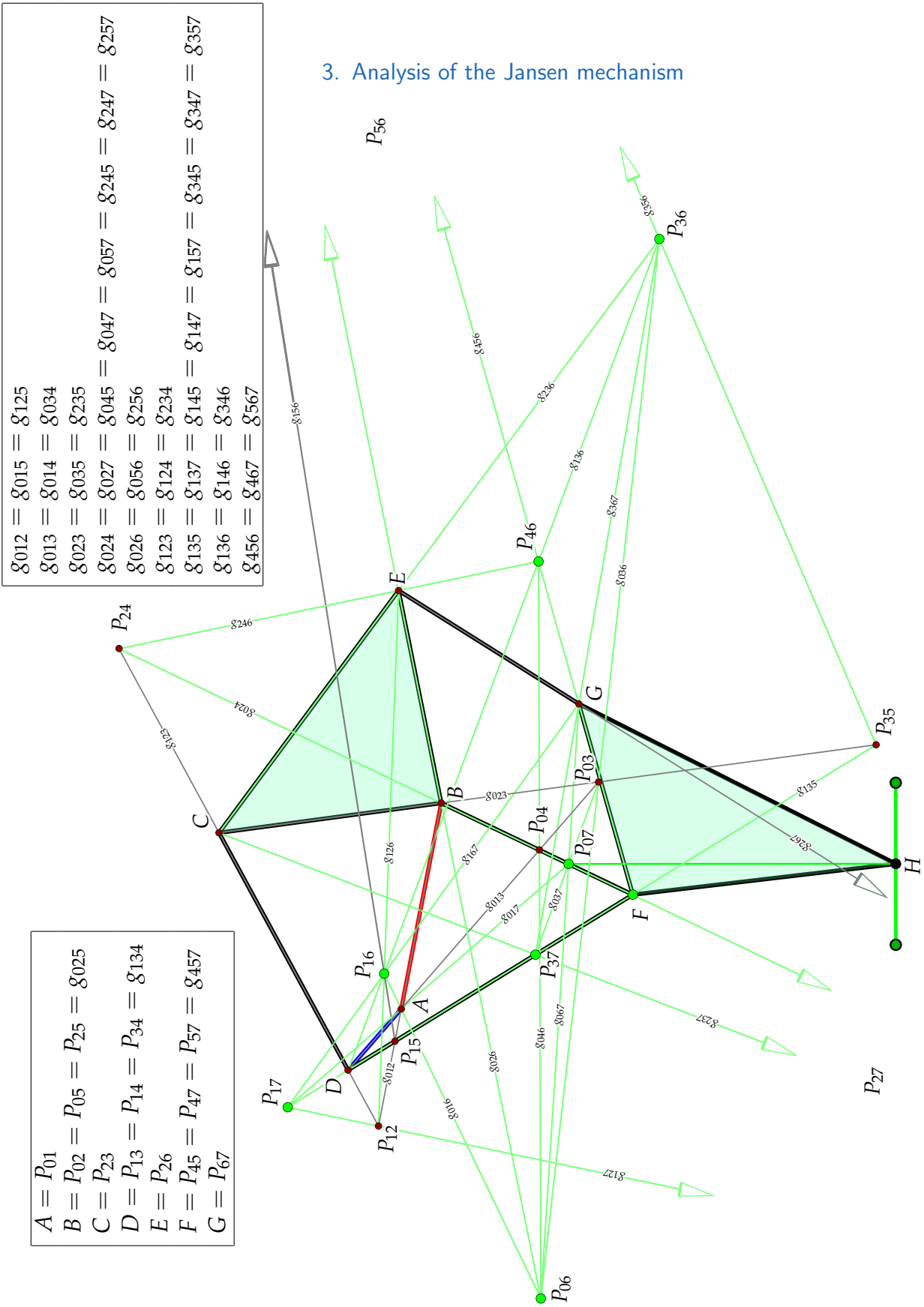


Figure 3.6.: ICR configuration of the Jansen mechanism

### 3. Analysis of the Jansen mechanism

In Fig. 3.7 we start by constructing the velocity of the point  $F$  with respect to the pole  $P_{04}$ . The velocity  $\mathbf{v}_{D,04}$  can be transferred to the point  $F$  to determine the velocity  $\mathbf{v}_{F,04}$ .

$$\mathbf{v}_{F,04} + \underbrace{\mathbf{v}_{F,A7}}_{=0} = \mathbf{v}_{F,07} \Rightarrow \mathbf{v}_{F,04} = \mathbf{v}_{F,07}.$$

The joint in  $F$  is a part of  $\Sigma_7$  and we know its velocity  $\mathbf{v}_{F,07}$  with respect to the base  $\Sigma_0$ . We can again transfer the angular velocity of  $F$  to the foot tip  $H$  and get  $\mathbf{v}_{H,07}$  as a result.

To confirm the construction, it is also possible to construct the velocities of the Jansen mechanism in the other direction, using the Systems  $\Sigma_2$  and  $\Sigma_6$  to have a connection from the crank to the foot. In Figure 3.7 this is illustrated in light green.

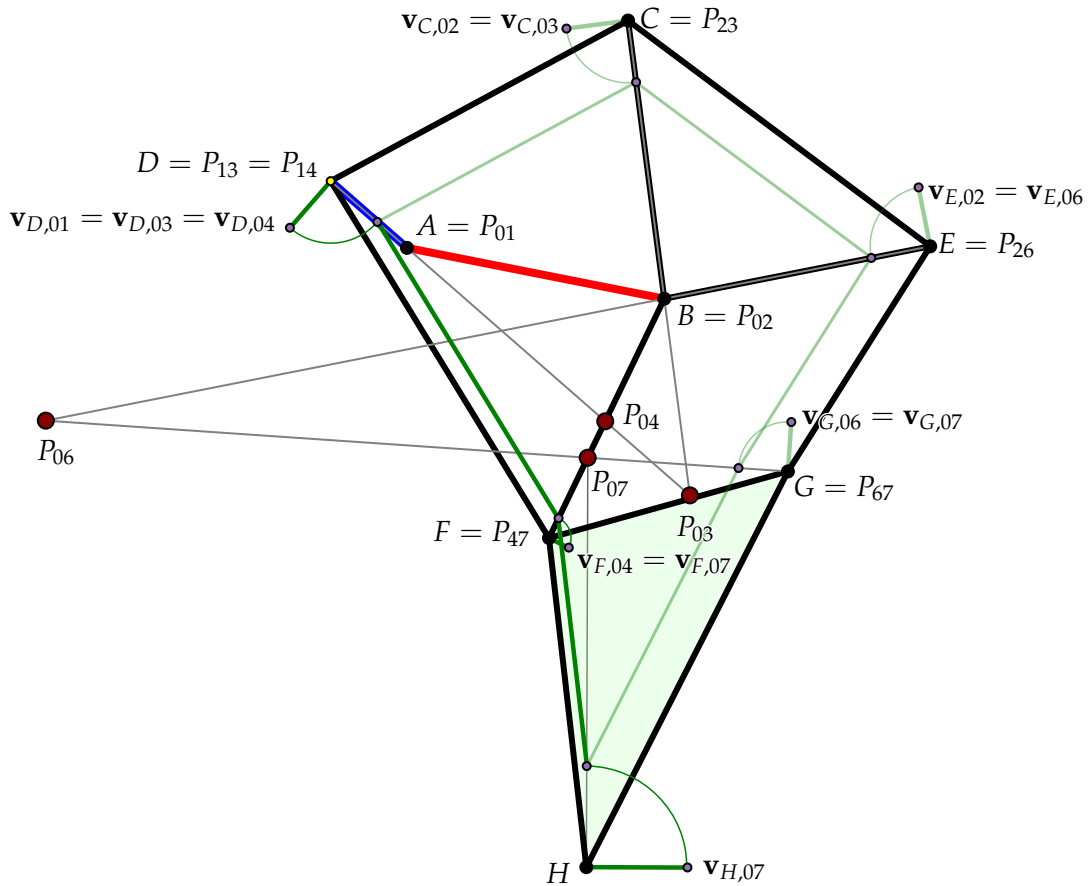


Figure 3.7.: Velocity distribution of the Jansen mechanism

### 3.4. Parametrization of the Jansen mechanism

As we have shown in section 3.1, the DOF of the Jansen mechanism is one, i.e. the Jansen mechanism is a one parametric mechanism. The crank gets driven with a constant velocity, therefore the angle  $\varphi$  can be interpreted as a value of time, thus the angle will be called  $t$ . Coordinate frames are placed in the systems of the Jansen mechanism, to calculate the position of each individual system at any time instance  $t$  (see Fig: 3.8). The position of the system  $\Sigma_7 \setminus \Sigma_0$  is of special interest.

The first of three four bar linkage is built up with the systems  $\Sigma_0, \Sigma_1, \Sigma_2, \Sigma_3$  and is the same as in the example of a four bar linkage (see Subsection 2.5). The length of the bars will be written as  $a_i, b_i, c_i, d_i$  with  $i = 1, 2, 3$  as used in the standard notation. The angles of the first four bar linkage are called  $\varphi_i$ , the angles of the second four bar linkage  $\psi_i$  and for the third four bar linkage  $\theta_i$  with  $i = 1, 2, 3$ .

The position of the coordinate frames in the first four bar linkage can be calculated as follows:

$$\Sigma_1 \setminus \Sigma_0 : \begin{pmatrix} 1 \\ x_0 \\ y_0 \end{pmatrix} = \underbrace{\begin{pmatrix} 1 & 0 & 0 \\ 0 & \cos(t) & -\sin(t) \\ 0 & \sin(t) & \cos(t) \end{pmatrix}}_{\mathbf{M}_{0,1}} \begin{pmatrix} 1 \\ x_1 \\ y_1 \end{pmatrix} \quad (3.1)$$

and

$$\Sigma_{2a} \setminus \Sigma_0 : \begin{pmatrix} 1 \\ x_0 \\ y_0 \end{pmatrix} = \underbrace{\begin{pmatrix} 1 & 0 & 0 \\ d_1 & \cos(\varphi_2) & -\sin(\varphi_2) \\ 0 & \sin(\varphi_2) & \cos(\varphi_2) \end{pmatrix}}_{\mathbf{M}_{0,2a}} \begin{pmatrix} 1 \\ x_{2a} \\ y_{2a} \end{pmatrix}, \quad (3.2)$$

with  $\varphi_2 = \varphi_2(t)$ . It is not necessary to compute a coordinate frame in the coupler in order to get all points of the mechanism.

For the first triangle, we will put a coordinate frame in  $\Sigma_{2b}$ . This happens by rotating in a negative direction with respect to the coordinate frame in  $\Sigma_{2a}$ . The angle  $\alpha$  is constant and can be calculated using the laws of cosines.

$$\Sigma_{2b} \setminus \Sigma_{2a} : \begin{pmatrix} 1 \\ x_{2a} \\ y_{2a} \end{pmatrix} = \underbrace{\begin{pmatrix} 1 & 0 & 0 \\ 0 & \cos(\alpha) & \sin(\alpha) \\ 0 & -\sin(\alpha) & \cos(\alpha) \end{pmatrix}}_{\mathbf{M}_{2a,2b}} \begin{pmatrix} 1 \\ x_{2b} \\ y_{2b} \end{pmatrix} \quad (3.3)$$

### 3. Analysis of the Jansen mechanism

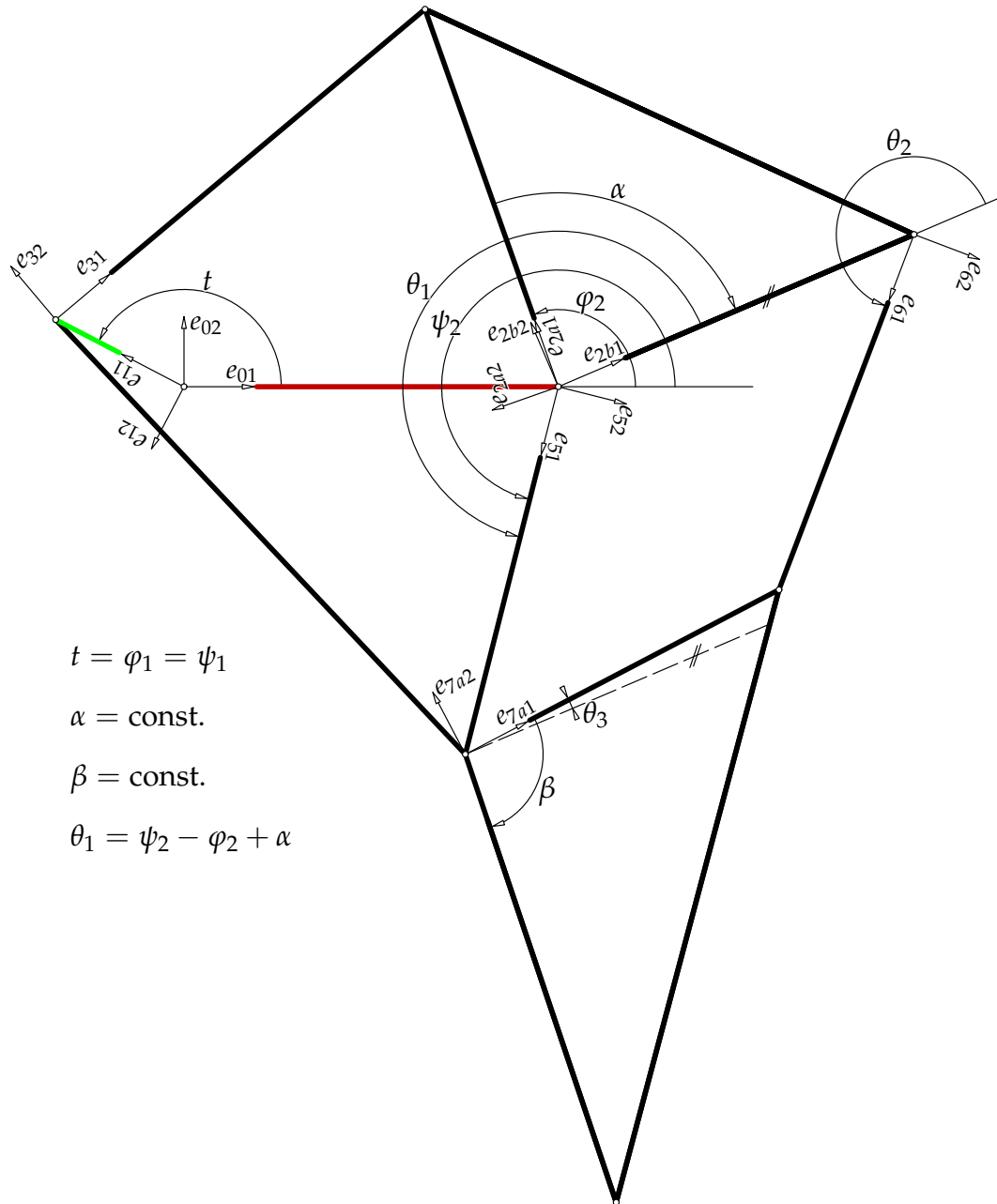


Figure 3.8.: Notation for the parametrization of the Jansen mechanism

### 3. Analysis of the Jansen mechanism

The second four bar linkage  $\Sigma_0, \Sigma_1, \Sigma_5, \Sigma_4$  uses the same drive angle  $t = \psi_1$ , therefore the position of the coordinate frame in  $\Sigma_1$  is unchanged. The position of  $\Sigma_5$  is the only one which has to be computed. The system  $\Sigma_4$  is the connection between the bars  $\Sigma_1$  and  $\Sigma_5$ .

$$\Sigma_5 \setminus \Sigma_0 : \begin{pmatrix} 1 \\ x_0 \\ y_0 \end{pmatrix} = \underbrace{\begin{pmatrix} 1 & 0 & 0 \\ d_1 & \cos(\psi_2) & \sin(\psi_2) \\ 0 & -\sin(\psi_2) & \cos(\psi_2) \end{pmatrix}}_{\mathbf{M}_{0,5}} \begin{pmatrix} 1 \\ x_5 \\ y_5 \end{pmatrix}, \quad (3.4)$$

with  $\psi_2 = \psi_2(t)$ .

The third four bar linkage consists of the systems  $\Sigma_5, \Sigma_6, \Sigma_{7a}, \Sigma_{2b}$  and the drive angle  $\theta_1$  is measured between the systems  $\Sigma_{2b}$  and  $\Sigma_5$ .  $\theta_1$  can be calculated as  $\theta_1 = \psi_2 - \varphi_2 + \alpha$ . The system  $\Sigma_{7a}$  is the coupler in that linkage, so this angle also has to be computed.

$$\Sigma_6 \setminus \Sigma_{2b} : \begin{pmatrix} 1 \\ x_{2b} \\ y_{2b} \end{pmatrix} = \underbrace{\begin{pmatrix} 1 & 0 & 0 \\ d_3 & \cos(\theta_2) & -\sin(\theta_2) \\ 0 & \sin(\theta_2) & \cos(\theta_2) \end{pmatrix}}_{\mathbf{M}_{2b,6}} \begin{pmatrix} 1 \\ x_6 \\ y_6 \end{pmatrix} \quad (3.5)$$

$$\Sigma_{7a} \setminus \Sigma_{2b} : \begin{pmatrix} 1 \\ x_{2b} \\ y_{2b} \end{pmatrix} = \underbrace{\begin{pmatrix} 1 & 0 & 0 \\ a_3 \cdot \cos(s) & \cos(\theta_3) & -\sin(\theta_3) \\ a_3 \cdot \sin(s) & \sin(\theta_3) & \cos(\theta_3) \end{pmatrix}}_{\mathbf{M}_{2b,7a}} \begin{pmatrix} 1 \\ x_{7a} \\ y_{7a} \end{pmatrix} \quad (3.6)$$

The last step in order to determine the position of the footpoint is to rotate the coordinate frame in  $\Sigma_{7a}$  in a negative direction by  $\beta$  degrees, which is the constant angle of the triangular shaped  $\Sigma_7$  in the corner where the coordinate frame is placed.

With the known position of system  $\Sigma_7$ , the coordinates of the footpoint are

$$\begin{pmatrix} 1 \\ x_7 \\ y_7 \end{pmatrix} = \begin{pmatrix} 1 \\ i \cdot \cos(\beta) \\ i \cdot \sin(\beta) \end{pmatrix}$$

with  $i$  is the distance from the origin of that coordinate frame to the footpoint. The position of the footpoint with respect to the coordinate frame

### 3. Analysis of the Jansen mechanism

$\{O_0; \mathbf{e}_{01}, \mathbf{e}_{02}\}$  is of special interest. This can be achieved by composition of previous motions as follows:

$$\Sigma_7 \setminus \Sigma_0 : \begin{pmatrix} 1 \\ x_0 \\ y_0 \end{pmatrix} = \underbrace{(\mathbf{M}_{0,2a} \cdot \mathbf{M}_{2a,2b} \cdot \mathbf{M}_{2b,7})}_{\mathbf{M}_{0,7}} \begin{pmatrix} 1 \\ x_7 \\ y_7 \end{pmatrix}, \quad (3.7)$$

The fixed base of the first two for bar linkages of a Jansen mechanism needs to be at a specific angle to result in a smooth walking motion. For easier calculation the fixed base was placed parallel to the x-axis. After calculating the position of all points, they have to be rotated in a clockwise direction by  $11,6^\circ$  around the origin. The locus of the foot tip is also turned and therefore the flat part appears to be parallel to the ground.

# Part II.

## Optimization

## 4. Optimization of the Jansen mechanism

This chapter is organized as follows: A brief introduction in genetic algorithms is given in Section 4.1 and in Section 4.2, a genetic algorithm is presented, that develops Jansen-style mechanisms whose loci meet any given locus.

### 4.1. Introduction to genetic algorithms

Theo Jansen found his holy numbers by what he described as an evolutionary method. Precise details about his work are not available, he used a computer but it seems that at least parts of the selection were done by hand.

As stated in [5], genetic algorithms (GAs) can be used to solve a great variety of problems. One application of genetic algorithms is to minimize a prescribed goal function  $F(\zeta_1, \dots, \zeta_n)$  with parameters  $\zeta_\tau, \tau = 1, \dots, n$ . In general the parameters have to fulfill constraints which can be a set of inequalities  $G_1(\zeta_\tau) < 0, \dots, G_m(\zeta_\tau) < 0$ . By varying the set of parameters a genetic algorithm reaches its goal. When the search space of the parameters  $\zeta_\tau$  is large or unknown or when the constraints  $G_\sigma, \sigma = 1, \dots, m$  are nonlinear, genetic algorithms get commonly used. A GA uses the following steps until predefined criteria are met:

1. **Initialization:** Create a random *population* with  $p$  inhabitants  $\mathbf{r}_\kappa = (r_{\kappa 1}, \dots, r_{\kappa n}), \kappa = 1, \dots, p$  which satisfy the constraints  $G_\sigma(\mathbf{r}_\kappa) < 0$ . The  $\mathbf{r}_\kappa$  are also called *chromosomes* and the  $r_{\kappa\tau}$  are called *genes*.
2. **Evaluation:** Calculate the *fitness*  $F(\mathbf{r}_\kappa)$  of each chromosome  $\mathbf{r}_\kappa$  in terms of the given objective function. This way the computer can differentiate between good or bad chromosomes.

## 4. Optimization of the Jansen mechanism

3. **Selection:** Regarding the fitness  $F(\mathbf{r}_\kappa)$ , the algorithm is more likely to select better chromosomes  $\mathbf{r}_\kappa$  for reproduction for the next generation.
4. **Recombination:** The selected chromosomes are called *parents*. A new *offspring* for the next generation is created by *crossover*. In the process of crossover the genes of the parents are usually combined randomly with certain restrictions, to create a new offspring.
5. **Mutation:** Changing one chromosome by modifying one or more genes slightly is called *mutation*. Mutation is done with a much lower probability than recombination.
6. **Replacement:** After recombination and mutation the algorithm checks, if the new chromosomes are still valid under the constraints  $G_\sigma$ . If so, the fitness  $F(\mathbf{r}_\kappa)$  of the new chromosomes is calculated and compared to the fitness of the chromosome of the previous generation. If the value of the fitness is lower in the new generation, the old chromosome will be replaced and takes the place in the population for the new generation, otherwise the old chromosome will stay in the population for the next generation.
7. Repeat steps 2 - 6 until a predefined goal is reached.

The run time of a genetic algorithm can vary noticeably depending on the population size or the maximum of generations which are run through.

### 4.2. Genetic algorithm for synthesizing a Jansen-style mechanism

In [1], a genetic algorithm was used to find the positioning and the lengths of the bars of a four bar mechanism with a triangular shaped coupler. The goal was that the end effector meets defined input points with further restrictions. We will adapt this algorithm to synthesize Jansen-style mechanisms whose end effector loci meet the locus of the foot of Jansen's mechanism. A different notation to Jansen's *Holy Numbers* will be used (see Table 4.1 and Fig. 4.1).

We define  $s$  positions  $(u_\rho, v_\rho)$ ,  $\rho = 1, \dots, s$  of the mechanisms foot tip  $H$  which are generated from the parametrization of the Jansen mechanism derived in Section 3.4. We also define the time instances  $t_\rho$ , for which the positions of  $(u_\rho, v_\rho)$  should be reached. We will generate a Jansen-style mechanism whose end effector tip approximates the points  $(u_\rho, v_\rho)$  while moving. The coordinates of the new mechanism's foot tip positions

#### 4. Optimization of the Jansen mechanism

Holy numbers	systems	new notations
$m^* = 15.0$	$\Sigma_1$	$a$
$b^* = 41.5$	$\Sigma_2$	$b$
$j^* = 50.0$	$\Sigma_3$	$c$
$n^* = \sqrt{a^{*2} + l^{*2}} \approx 38.8$	$\Sigma_0$	$d$
$c^* = 39.3$	$\Sigma_5$	$e$
$k^* = 61.9$	$\Sigma_4$	$f$
$d^* = 40.1$	$\Sigma_2$	$g$
$e^* = 55.8$	$\Sigma_2$	$h$
$f^* = 39.4$	$\Sigma_6$	$i$
$g^* = 36.7$	$\Sigma_7$	$j$
$i^* = 49.0$	$\Sigma_7$	$k$
$h^* = 65.7$	$\Sigma_7$	$l$
with $l^* = 7.8$ $a^* = 38.0$		
Positioning of the mechanism		
$x^* = 0$		$x_A$
$y^* = 0$		$y_A$
$\gamma^* = \arctan(l^*/a^*) = 11.6^\circ$		$\gamma$

Table 4.1.: Notations of the Jansen mechanism and the notation for the GA

#### 4. Optimization of the Jansen mechanism

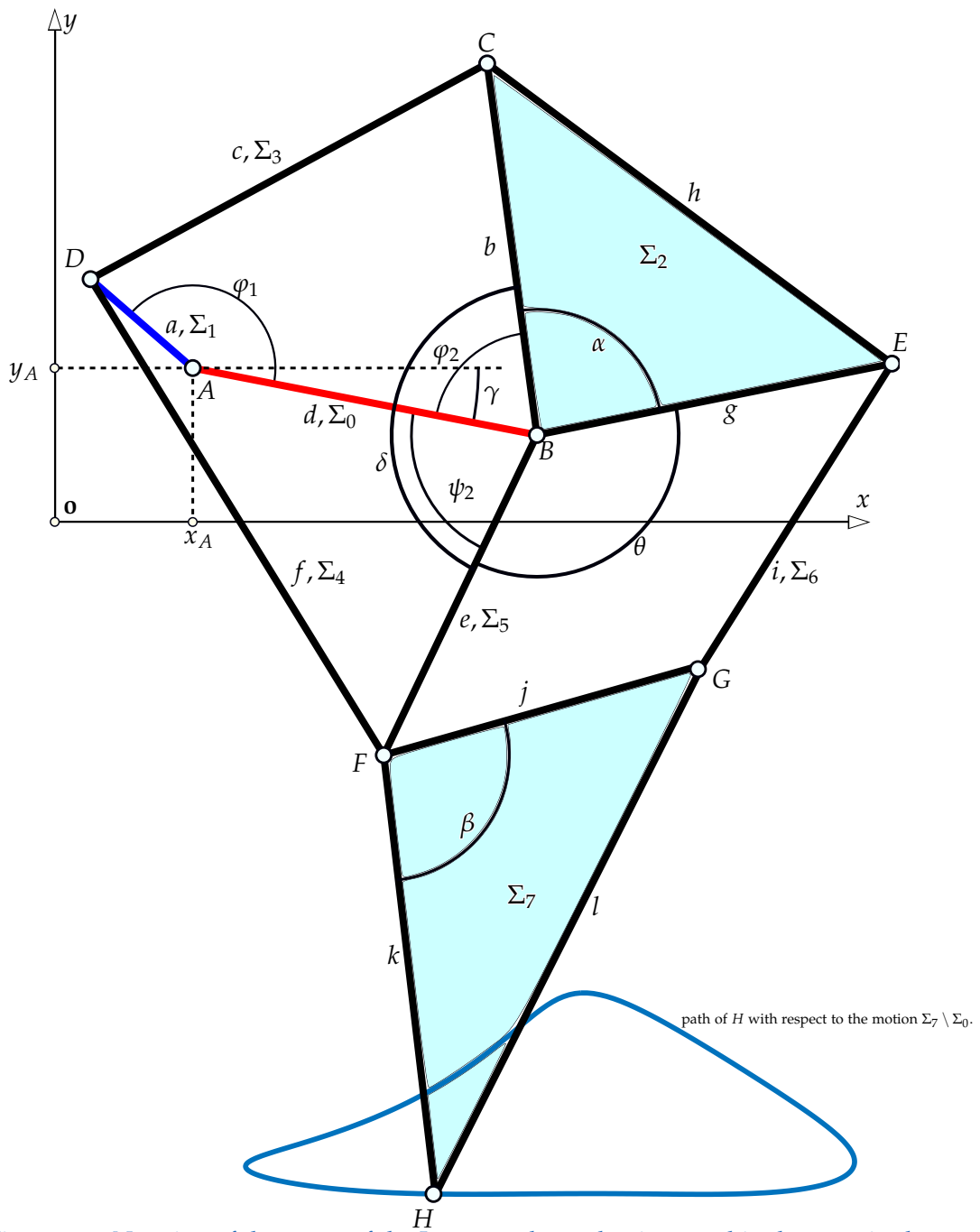


Figure 4.1.: Notation of the genes of the Jansen-style mechanism used in the genetic algorithm

## 4. Optimization of the Jansen mechanism

belonging to the time instances  $t_\rho$  will be denoted by  $(\xi_\rho, \eta_\rho)$ . Hence, the goal function  $F$  to be minimized will be

$$F(\xi_\rho, \eta_\rho) := \sum_{\rho=1}^s \left( (\xi_\rho - u_\rho)^2 + (\eta_\rho - v_\rho)^2 \right).$$

### 4.2.1. Starting population

This subsection is about the initialization as described in Section 4.1. Initially we generated the lengths of the bars simply with random numbers until they met our restriction. It worked out but was not very effective, so we looked for a way to generate valid lengths straight forward. A quite complex way was found, but due to clustering in the results this approach had to be discharged and it was back to the random numbers. The main difference to [1] is that due to the different architecture of the leg mechanism also nonlinear constraints are necessary.

We start by creating a population of  $p$  chromosomes, where each chromosome represents a mechanism. Each chromosome is built up of 15 *genes*. The first 12 genes represent the lengths  $a, b, \dots, l$  of the mechanism's bars and the other three hold the  $x, y$ -position of the point  $A = (x_A, y_A)$  and the angle  $\gamma$  of the bar  $AB$  against the  $x$ -axis of the coordinate system (see Fig. 4.1).

To generate a valid starting population we split the whole mechanism into parts. Once the values of the genes of the first part are known, we can move on to the next part and use these values for further restrictions and so on.

To restrict the overall size of the mechanism, we only choose values of the genes in a predefined interval  $[q_0, q_1]$  with exceptions of the genes  $h$  and  $l$ . This is because of the way these values are chosen - a greater variety of mechanisms is possible by canceling these limitations.

#### Selection of the parameters $a, b, c, d, e, f$ of the starting population

The first six chromosomes hold the values of the lengths of two four bar linkages.

#### 4. Optimization of the Jansen mechanism

The first four genes  $a, b, c, d$  of each chromosome represent the first four bar mechanism  $(\Sigma_0, \Sigma_1, \Sigma_2, \Sigma_3)$ . We want to generate mechanisms, where  $\Sigma_1$  serves as a crank and therefore a full revolution around the point  $A$  has to be possible. The gene  $a$  represents the length of the crank  $\Sigma_1$ ,  $\Sigma_2$  is the second arm with length  $b$ ,  $\Sigma_3$  is the coupler with length  $c$  and  $d$  holds the length of the base  $\Sigma_0$ . To check if a four bar linkage or a triangle is possible to build, we have to verify that the length of any bar is shorter than the sum of the lengths of the other bars. According to [2, p. 29], a full revolution in a joint of a four bar linkage is possible, if the sum of the lengths of one of the bars, for instance  $a^1$ , connected in this joint with any other bar is shorter or equal than the sum of the other two bars. This is equivalent to  $a + b \leq c + d$ ,  $a + c \leq b + d$ ,  $a + d \leq b + c$ . These three equations also imply that the bar  $a$  is the shortest of the mechanism.

The second four bar linkage  $(\Sigma_0, \Sigma_1, \Sigma_5, \Sigma_4)$  with  $\Sigma_5$  and  $\Sigma_4$  with lengths  $e$  and  $f$  also needs to have a crank in  $A$ , therefore the requirements are identical.

In total the following 12 linear constraints are necessary for the two four bar linkages:

$$q_0 \leq a \text{ and } b, \dots, e \leq q_1 \quad (4.1)$$

$$a + b - c - d \leq 0 \quad (4.2)$$

$$a - b + c - d \leq 0 \quad (4.3)$$

$$a - b - c + d \leq 0 \quad (4.4)$$

$$a + e - f - d \leq 0 \quad (4.5)$$

$$a - e + f - d \leq 0 \quad (4.6)$$

$$a - e - f + d \leq 0 \quad (4.7)$$

When generating the values, they are chosen randomly in the interval  $[q_0, q_1]$  that the first 6 equations 4.1 hold under any circumstances. This can be guaranteed by choosing  $a \in [q_0, q_1]$  and  $b, c, d, e, f \in [a, q_1]$  Afterward the equations 4.2 - 4.7 are checked. If the values pass all equations they will be kept for a mechanism, otherwise the values will be discharged and new values will be chosen. This method of eventually rejecting all values is called *rejection sampling*.

---

<sup>1</sup>A full revolution at joint  $A$  would also be feasible, if  $d + a \leq b + c$ ,  $d + b \leq a + c$ ,  $d + c \leq a + b$  hold, but since the original Jansen mechanism uses  $a$  as shortest length of the first and second four bar linkage, we will use the same approach.

#### 4. Optimization of the Jansen mechanism

##### Selection of the parameters $g, h$ of the starting population

The system  $\Sigma_2$  is represented by a triangle with edge lengths  $b, g, h$ . The value of the gene  $b$  is given and we randomly choose values for the angle  $\alpha$  (see Fig. 4.1) and the value  $g$ , the value of the gene  $h$  is calculated afterward. The angle  $\alpha$  is chosen so, that  $0 < \varphi_2 + \psi_2 + \alpha < 2\pi$  is true for all input angles  $\varphi_1$ . Since  $\alpha$  is a constant angle we will have to check the minimum and maximum of the angle  $\delta = \varphi_2 + \psi_2$  to verify, that the previous inequalities are valid. The value of  $g$  is chosen within the global limitations  $g \in [q_0, q_1]$ . With the law of cosine and the values for  $b, g$  and  $\alpha$ , the value of  $h$  can be calculated. For  $h$  the limitations  $q_0 \leq h \leq q_1$  were discharged, since if the value of  $b$  was getting close to  $q_1$ , it was nearly impossible to find valid values for  $\alpha$  and  $g$  that  $h$  was also valid. Even though the limits were discharged, the value of  $h$  can not exceed  $2 \cdot q_1$ .

**Proposition 1.** *The minimum of  $\delta = \varphi_2 + \psi_2$  is reached with the input angle  $\varphi_1 = \pi$  and the maximum at  $\varphi_1 = 0$*

**Proof.** For the extremal positions of  $\delta$  we have to find the input angles  $\varphi_1$  so, that  $\dot{\delta} = \omega_{25} = 0$ . By

$$\mathbf{v}_{C,02} + \mathbf{v}_{C,25} = \mathbf{v}_{C,05}$$

we have

$$\mathbf{v}_{C,25} = \mathbf{v}_{C,05} - \mathbf{v}_{C,02}. \quad (4.8)$$

As  $\delta$  is extremal,  $\mathbf{v}_{25}$  has to be  $\mathbf{o}$ . Hence, due to 4.8

$$\mathbf{v}_{C,02} = \mathbf{v}_{C,05}.$$

must hold.

We still need to show that  $\mathbf{v}_{C,25} = \mathbf{o}$  when  $\varphi_1 = 0$  and  $\varphi_1 = \pi$ , i.e.

$\varphi_1 \in \{0, \pi\} \Rightarrow \mathbf{v}_{C,02} = \mathbf{v}_{C,05}$ . By looking at the ICR configuration of the mechanism it is easy to see that in these two positions many poles coincide, which can be verified in Fig. 4.2 and 4.3 and therefore it is obvious to see that the angular velocities  $\omega_{02}$  and  $\omega_{05}$  of the motions  $\Sigma_2 \setminus \Sigma_0$  and  $\Sigma_5 \setminus \Sigma_0$  are identical.  $\square$

**Remark 2.** The angle  $\theta$  (see Fig 4.1) is given as  $\theta = 2\pi - \delta - \alpha$  and therefore we know that

$$\delta_{min} \longleftrightarrow \theta_{max} \text{ and } \delta_{max} \longleftrightarrow \theta_{min}.$$

#### 4. Optimization of the Jansen mechanism

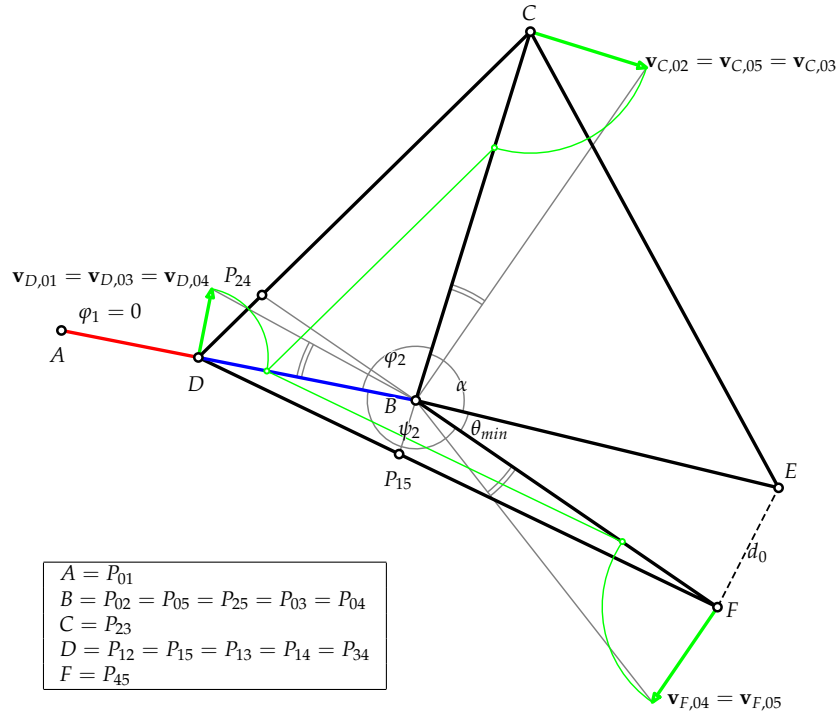


Figure 4.2.: Minimum of the angle  $\theta$

#### Selection of the parameters $i, j$ of the starting population

The third four bar linkage ( $\Sigma_5, \Sigma_6, \Sigma_7, \Sigma_2$ ) is represented by the parameters  $(e, i, j, g)$ . The values of  $e$  and  $g$  and also the minimum and maximum of the angle  $\theta$  are already known. With  $\theta$  and the law of cosine, we can calculate the minimum  $d_0$  and the maximum  $d_1$  of the diagonal  $EF$  of the quadrilateral  $BEGF$ :  $d_0 = \sqrt{e^2 + g^2 - 2eg \cdot \cos \theta_{min}}$  and  $d_1 = \sqrt{e^2 + g^2 - 2eg \cdot \cos \theta_{max}}$  (see Fig. 4.2 and Fig. 4.3).

We aim to find  $i$  and  $j$  so that the four bar linkage is constructable and non-crossed in all positions. The constraints on the parameters are as follows, see Fig. 4.4:

1.  $q_0 < i, j < q_1$  (limitations of the length)
2. The triangles  $(i, j, d_0)$  and  $(i, j, d_1)$  are constructable
3.  $\mu_1 < \pi - \lambda_1$  and  $\mu_2 < \pi - \lambda_2$  (non-crossing condition)

1 and 2 yield four linear constraints, whereas 3 results in non-linear ones, see below. We give a graphical interpretation as we go through the steps with a coordinate system where the parameters  $i$  and  $j$  are interpreted as the coordinate frame. The shaded area of the following graphics represent all the valid positions of a point with coordinates  $(i, j)$  up to each step.

#### 4. Optimization of the Jansen mechanism

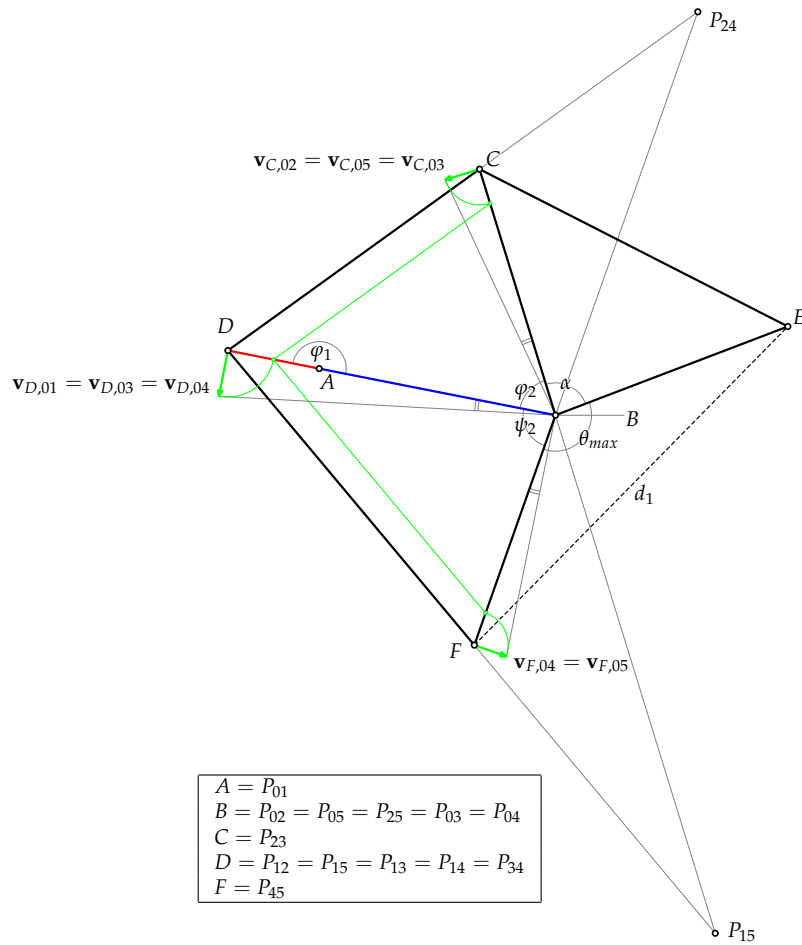


Figure 4.3.: Maximum of the angle  $\theta$

#### 4. Optimization of the Jansen mechanism

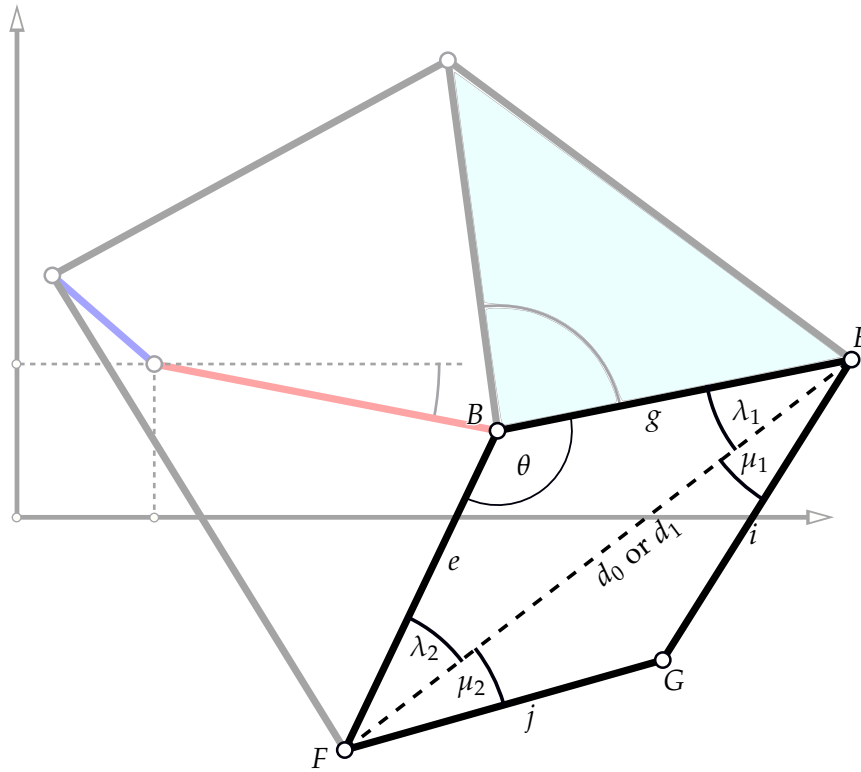


Figure 4.4.: Restrictions of the third FBL in the GA

Ad 1:

The values of the parameters are only valid within the general limitations  $[q_0, q_1]$ . This results in a square in the first quadrant with corners  $(q_0/q_0), (q_1/q_0), (q_1/q_1), (q_0/q_1)$ , see Fig. 4.5.

Ad 2:

Applying the triangle inequality on the triangles  $(i, j, d_0)$  and  $(i, j, d_1)$  results in six inequalities but due to  $d_0 < d_1$ , only three are essential:

$$\begin{array}{l|l} \cancel{i+j > d_0} & i+j > d_1 \\ \cancel{i+d_0 > j} & \cancel{i+d_1 > j} \\ \cancel{j+d_0 > i} & \cancel{j+d_1 > i} \end{array} \implies \begin{array}{l} j > -i + d_1 \\ j < i + d_0 \\ j > i - d_0 \end{array}$$

In the  $i, j$ -plane these three inequalities characterize three half planes (see Fig. 4.6). The half planes may cut three corners of the square from 1 to further restrict the possible values of the parameters  $i$  and  $j$ .

Ad 3:

For the nonlinear part, we check the angles of the triangles from 2 that

#### 4. Optimization of the Jansen mechanism

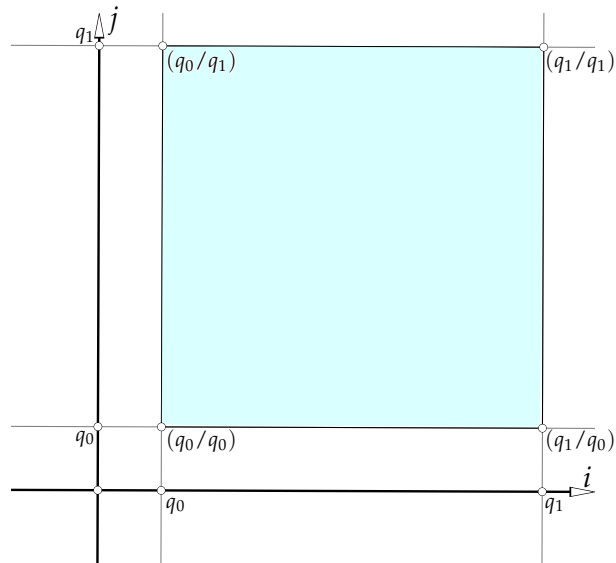


Figure 4.5.: Step 1 of finding parameters  $i, j$

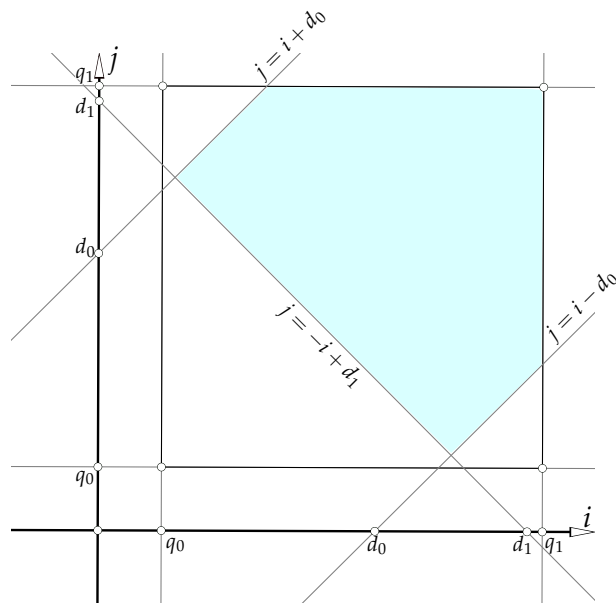


Figure 4.6.: Step 2 of finding parameters  $i, j$

#### 4. Optimization of the Jansen mechanism

they stay within their limits. We only have to check these constraints for the shorter diagonal  $d_0$ . The crossing of the systems first occurs in the minimal position of  $\theta$ , if there is crossing at all. The angle  $\mu_1$  between  $d_0$  and  $i$  can be calculated with the law of cosines as follows:

$$\begin{aligned} j^2 &= i^2 + d_0^2 - 2 i d_0 \cos \mu_1 \\ \cos \mu_1 &= \frac{i^2 + d_0^2 - j^2}{2 i d_0} \end{aligned} \quad (4.9)$$

To avoid crossed states of the quadrilateral  $BGEF$  we have to limit the angle  $\mu_1$ :

$$\mu_1 < \pi - \lambda_1 \Leftrightarrow \cos \mu_1 > \cos(\pi - \lambda_1) \Leftrightarrow \cos \mu_1 > -\cos \lambda_1.$$

Using 4.9 means:

$$\begin{aligned} j^2 - i^2 - 2 i d_0 \cos \lambda_1 - d_0^2 &< 0 \\ \Leftrightarrow \\ j^2 - (i^2 - 2 i d_0 \cos \lambda_1 + d_0^2 \cos^2 \lambda_1) - d_0^2 + d_0^2 \cos^2 \lambda_1 &< 0 \\ \Leftrightarrow \\ j^2 - (i + d_0 \cos \lambda_1)^2 + d_0^2 \underbrace{(-1 + \cos^2 \lambda_1)}_{=-\sin^2 \lambda_1} &< 0 \\ \Leftrightarrow \\ j^2 - (i + d_0 \cos \lambda_1)^2 - d_0^2 \sin^2 \lambda_1 &< 0 \end{aligned}$$

The last line represents the *interior* of a hyperbola centered in  $(-d_0 \cos \lambda_1/0)$ , whose vertices are  $(-d_0 \cos \lambda_1/ \pm d_0 \sin \lambda_1)$  and whose asymptotes are parallel to the 1<sup>st</sup> and 2<sup>nd</sup> median, see Fig. 4.7. The hyperbola and its asymptotes are plotted in blue.

Similar considerations can be done for the second non-crossing condition  $\mu_2 < \pi - \lambda_2$  from 3. This results in  $i^2 - (j + d_0 \cos \lambda_2)^2 - d_0^2 \sin^2 \lambda_2 < 0$  the interior of a hyperbola  $(0/ -d_0 \cos \lambda_2)$  whose vertices are  $(\pm d_0 \sin \lambda_2/ -d_0 \cos \lambda_2)$ . The asymptotes are also parallel to the 1<sup>st</sup> and 2<sup>nd</sup> median. This hyperbola cuts a part off the lower part of the shaded area in Fig. 4.8. The hyperbola and its asymptotes are plotted in brown.

With the known borders of the area we can start generating a random point inside the area, this method is known as rejection sampling. Therefore we circumscribe an axis parallel rectangle around the calculated area and

#### 4. Optimization of the Jansen mechanism

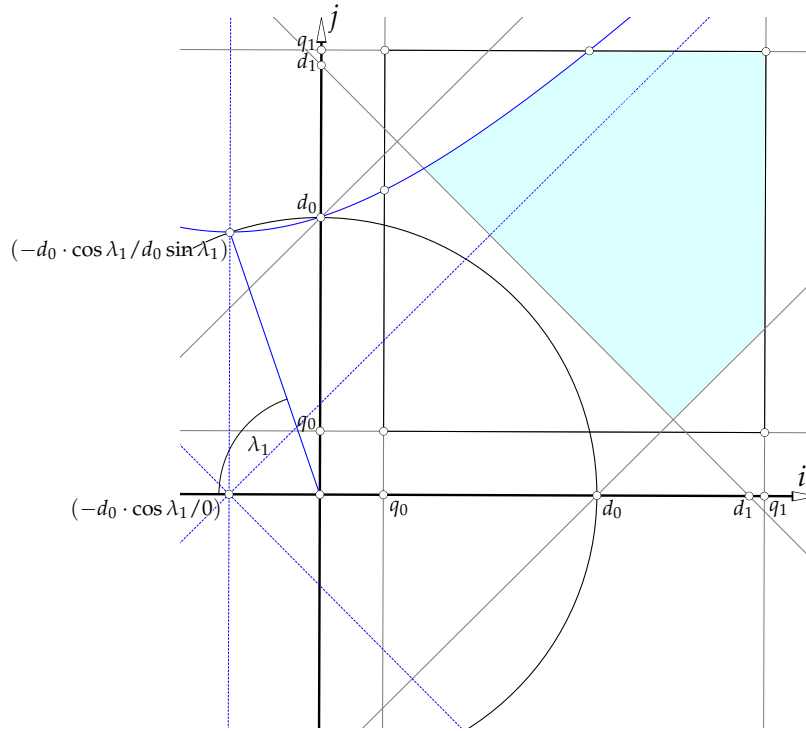


Figure 4.7.: Step 3 of finding parameters  $i, j$

choose a random point inside this rectangle. The coordinates representing the values for  $i$  and  $j$  are checked if they are inside the shaded area, in other words if they are valid (see Fig. 4.8). If so, they will be kept, otherwise the values will be discharged and new values  $i, j$  will be generated.

#### Selection of the parameters $k, l$ of the starting population

As the foot of the mechanism, the triangle  $\Sigma_7$  represented by the parameters  $j, k, l$  is added. The value of  $j$  is already known, therefore only the other two parameters have to be chosen. At first, the angle  $\beta$  will be chosen in the interval  $(0, \pi)$ . The value of the parameter  $k$  is also randomly chosen in the interval  $[q_0, q_1]$ . With the law of cosine, the value of  $l$  is then calculated. Similar to the gene  $h$ , we do not use an upper limitation for  $l$  in order to not restrict the solutions too much.



#### 4. Optimization of the Jansen mechanism

$$F(a, \dots, l, x_A, y_A, \gamma) = \sum_{\rho=1}^s \left[ (\xi_{\rho} - u_{\rho})^2 + (\eta_{\rho} - v_{\rho})^2 \right] \quad (4.10)$$

with

$$\begin{pmatrix} 1 \\ \xi_{\rho} \\ \eta_{\rho} \end{pmatrix} = \mathbf{M}(t_{\rho}) \cdot \begin{pmatrix} 1 \\ k \cdot \cos(\beta) \\ k \cdot \sin(\beta) \end{pmatrix}, \quad (4.11)$$

$$\mathbf{M}(t_{\rho}) = \mathbf{M}_{0,2a}(t_{\rho}) \cdot \mathbf{M}_{2a,2b}(t_{\rho}) \cdot \mathbf{M}_{2b,7}(t_{\rho}) \quad \text{from 3.7 and} \quad (4.12)$$

$$\cos(\beta) = \frac{j^2 + k^2 - l^2}{2jk}, \quad \sin(\beta) = \sqrt{1 - \cos^2(\beta)} \quad (4.13)$$

#### 4.2.2. Selection, recombination, mutation and replacement

Since our goal is to minimize the distances to our target points, we sort the population according to its fitness from lowest to highest. Our ambition is to generate the next population by crossover or mutation of each chromosome and progressively decrease its fitness.

For each chromosome we generate a disturbance vector  $V$  by combining the best chromosome  $\mathbf{r}_{best}$  of the previous generation with two arbitrary chromosomes  $\mathbf{r}_1$ ,  $\mathbf{r}_2$  of the previous generation.  $\mathbf{r}_1$  and  $\mathbf{r}_2$  are selected by normalized distribution so that better chromosomes are more likely to be chosen. This method is known as *differential evolution* and  $V$  is calculated as

$$V = \mathbf{r}_{best} + M(\mathbf{r}_1 - \mathbf{r}_2),$$

with a constant  $M \in [0, 1]$ , which influences to what extent the best Chromosome  $X_{best}$  is disturbed.

A chromosome gets selected for crossover with a predefined crossover-probability  $CP \in [0, 1]$ , if selected, we choose the chromosome itself and the disturbance Vector  $V$  as parents. With *two point crossover* their offspring is generated as shown in Figure 4.9. The crossover points, where parts of each parents are selected, are chosen randomly. Therefore the genes and the length of the part which is selected from  $V$  varies. The fitness of the offspring is then calculated and if it is better than the fitness of its parent, the new offspring is chosen for the next generation.

Mutation happens independent of crossover and with a lower probability  $MP \in [0, 1]$ . For mutation a single gene of the chromosome is selected and

#### 4. Optimization of the Jansen mechanism

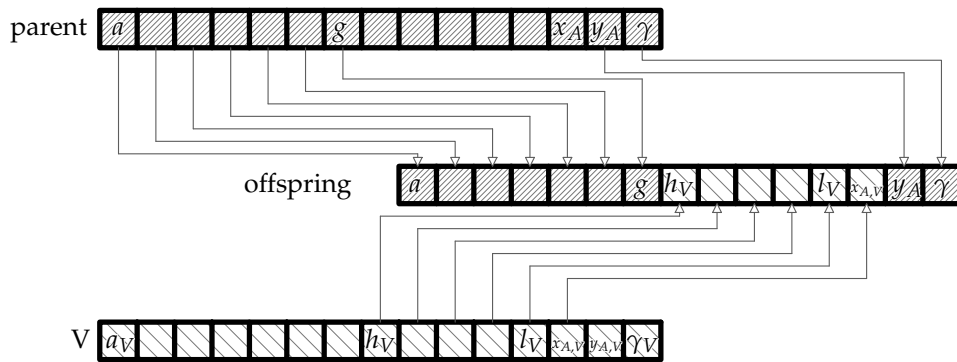


Figure 4.9.: Two point crossover

a random real number within a specified range is added '+' and subtracted '-' from it. The fitness of both new chromosomes ('+' and '-') is calculated and the fittest of the three chromosomes ('old', '+', '-') is selected for the next generation.

The previous steps are repeated until all chromosomes of one population are processed and then the whole procedure starts over for the next generation. Some chromosomes may not be changed at all from one generation to the next.

#### 4.2.3. End of algorithm

The algorithm stops either when the fitness of a chromosome is lower than a predefined threshold  $errmin$  or the number of generations exceeds a predefined integer value  $genmax$ . The flowchart in Fig. 4.10 shows the main structure of the algorithm.

#### 4. Optimization of the Jansen mechanism

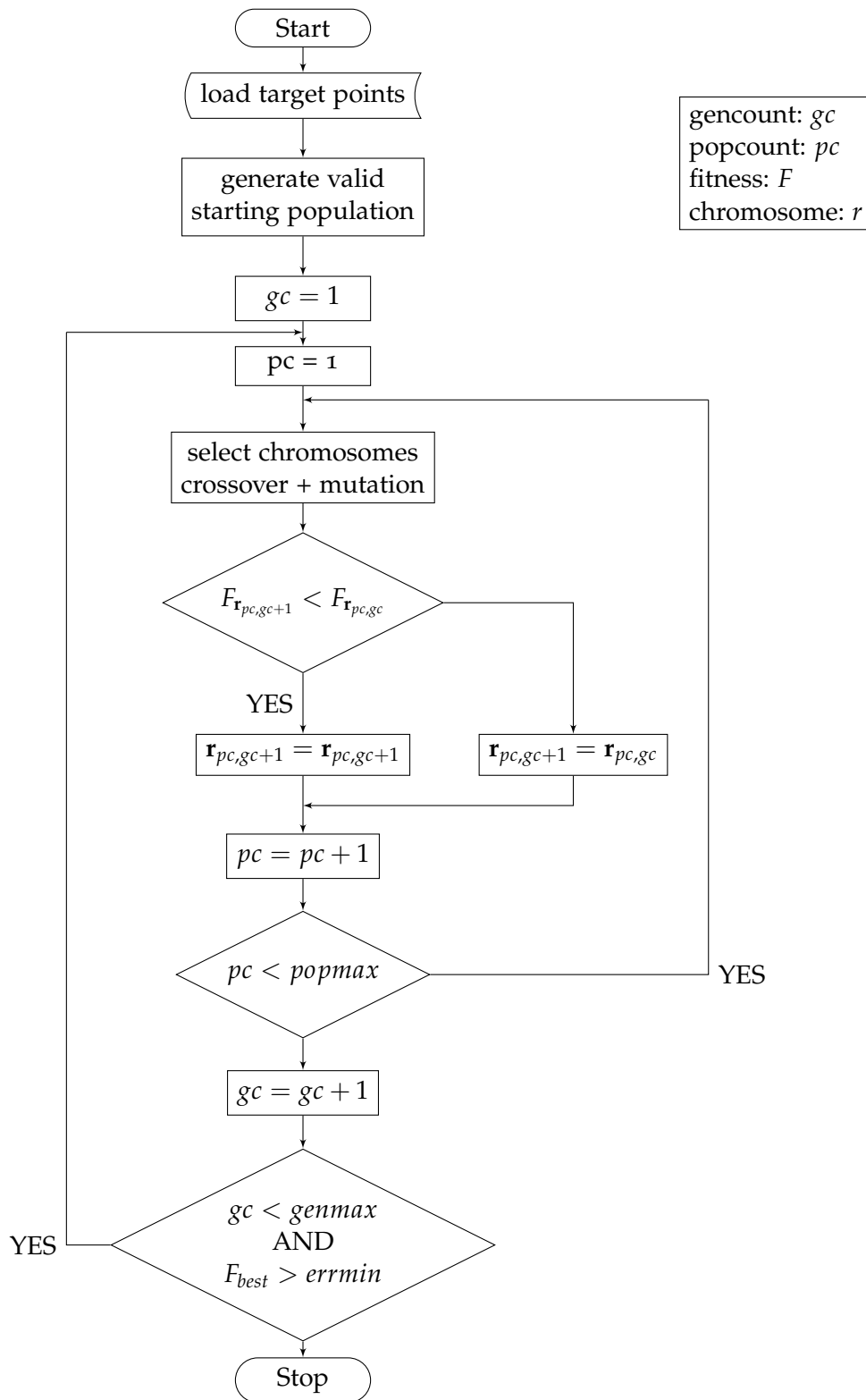


Figure 4.10.: Flowchart of the genetic algorithm

## 5. Results of the genetic algorithm

The genetic algorithm was tested by varying of different parameters. The focus was on changing the value  $M$  occurring in the disturbance vector  $V$ , the values  $CP$  and  $MP$  of the probabilities for crossover and mutation, the size of the population  $popmax$  and the maximum of generations  $genmax$  which were run through.

For  $M$ , values between 0.1 and 0.4 were tested. Lower values led to very small improvements but the mechanism kept improving up to high generations. The shape of the mechanism was not significantly changed during this process. With higher values for  $M$ , the mechanisms improved very much at the beginning, but stagnated towards the end of the evolution.

The crossover probability was tested for values  $CP \in [0.8, 0.9]$  and the mutation probability for values  $MP \in [0.2, 0.4]$ . The results were for any combinations of these values not better or worse in any way. Regarding the population size  $popsize$ , 200 mechanisms turned out to be the minimum number of mechanisms to reach the set goal, but in most tests 250 mechanisms were used. By looking at the graphs of the error reduction (see Figure 5.2), 2000 generations seemed to be a reasonable maximum number. Most error curves flattened out at that point.

The final results vary in size and shape, so different results are presented in four categories. Each category is represented in a separate section. In Section 5.1 mechanisms whose shape is close to the Jansen mechanism are illustrated. Section 5.2 is devoted to mechanisms with a reverse position of two bars connected to the crank which will be called *inverse mechanisms*. In Section 5.3 mixed mechanisms of the previous categories are presented and in Section 5.4 an infeasible result is shown, namely the two further categories of mechanisms.

The error was measured in absolute values and in the scale which was used, an error of  $s/2$  was aimed for, with  $s$  being the *number of target points* respectively steps, which was used. The error was also calculated as a percentage value of the error reduction compared to the best mechanism

## 5. Results of the genetic algorithm

of the starting population, but since the first mechanism was arbitrary, that number was not very significant.

### 5.1. Results close to the Jansen mechanism

The main goal of the genetic algorithm was to generate mechanisms close or similar to the Jansen mechanism. For a better understanding, 12 steps of an animation of the Jansen mechanism can be seen in Fig. 5.1. In the first step the angle of the crank is at zero degrees compared to the fixed base. To achieve a full revolution of the crank in 12 steps, the input angle was successively increased by 30 degrees for the next sub figure.

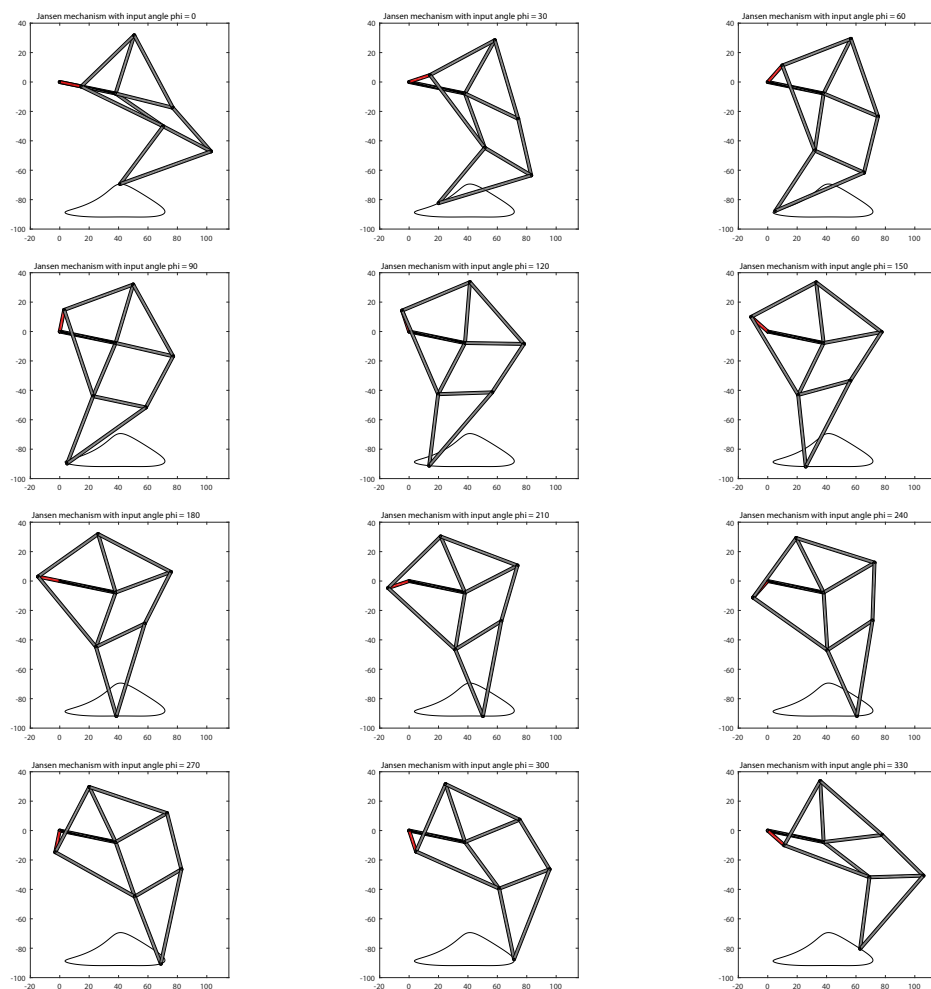


Figure 5.1.: Animation of the Jansen mechanism

## 5. Results of the genetic algorithm

Approximately 27 % of all generated mechanisms were close to the looks of the Jansen mechanism. This means that the two bars, represented by the genes  $c$  and  $f$  connected to the crank other than the fixed base are pointing towards the right when the crank is in the zero position. Also the lowest triangle with the foot is pointing from the right towards the locus. One resulting mechanism which was close to the Jansen mechanism is presented in more detail. At first a few generations will be shown, to see how the mechanism evolved. Afterwards the result is shown in a large image in comparison to the Jansen mechanism and also twelve steps of an animation are plotted. The following parameters were used in all tests:

- Design variables:  $a \dots l, x_A, y_A, \gamma$
- Target points: 12 points of the locus of the Jansen mechanism starting at an input angle of  $0^\circ$  and a step size of  $30^\circ$ .
- Limits of the variables:  $a, \dots, g$  and  $i, \dots, k \in [q_0, q_1] = [10, 70]$ ,  $h, l \in [q_0, 2q_1] = [10, 140]$ ,  $x_A, y_A \in [2q_1, 2q_1] = [-140, 140]$ ,  $\gamma \in [0, 2\pi]$ .

For each mechanism which is presented, only the variable parameters are listed. For the first result, the following parameters were used:

- $popsize = 250$ ,  $genmax = 2000$ ,  $CP = 0.9$ ,  $MP = 0.3$ ,  $M = 0.4$  and the allowed  $error = s/2 = 12/2 = 6$ .

In Figure 5.3 the evolution of the mechanism is presented. In the 250th generation, the mechanism was already close to the final dimensions but as can be seen in Fig. 5.2 the remaining error was decreased close to the 2000<sup>th</sup> generation.

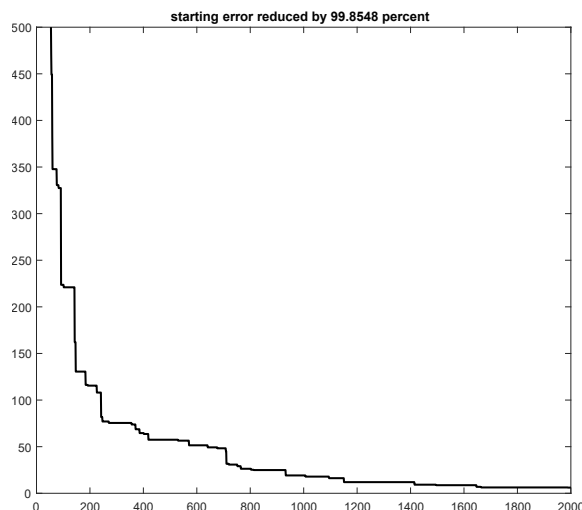


Figure 5.2.: Error reduction of genetic algorithm

## 5. Results of the genetic algorithm

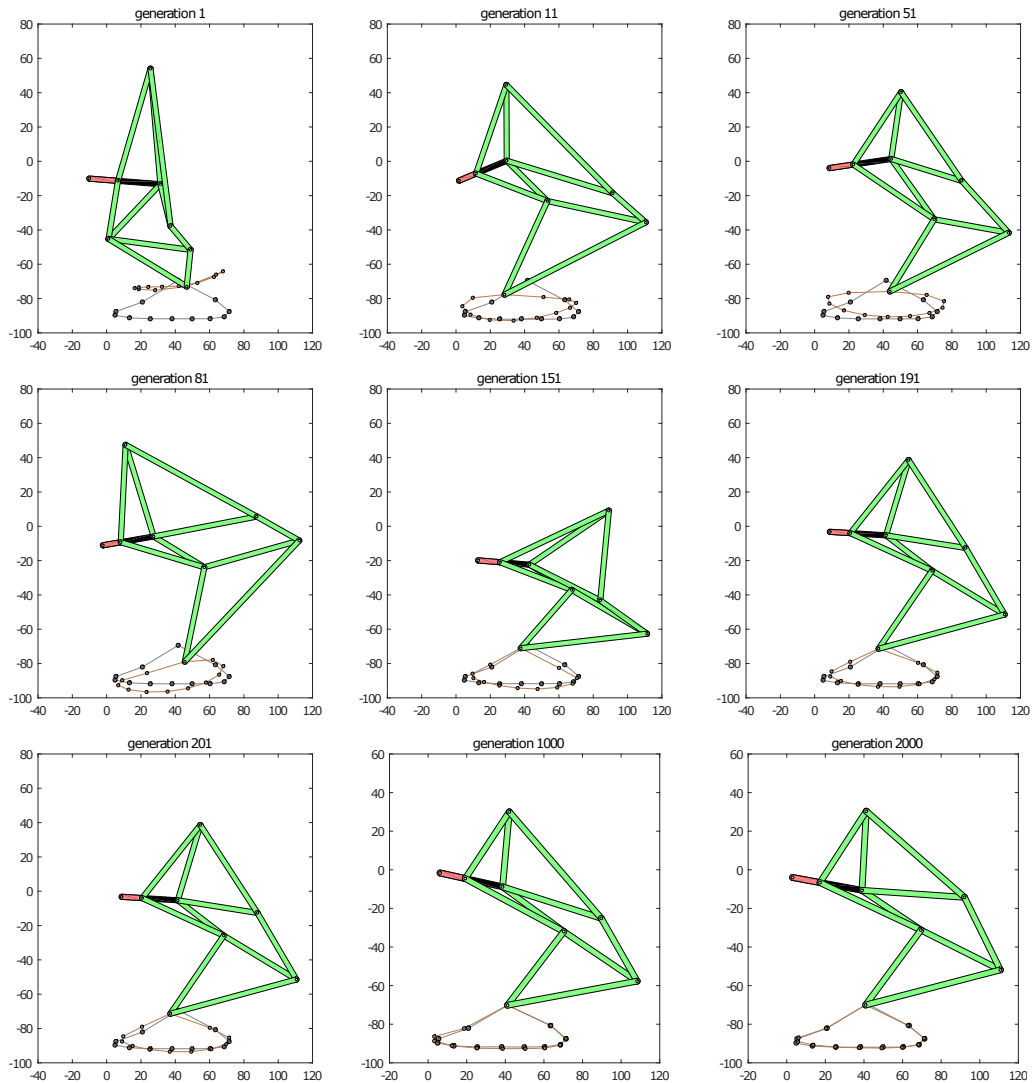


Figure 5.3.: Evolving of a mechanism through generations

This mechanism was chosen mainly because of its looks. The final minimized error turned out to be  $error = 6.0984$  which just did not reach the goal but was close enough. The algorithm was implemented in MATLAB and with an Intel(R) Core(TM) i5-3317U CPU @ 1.70GHz processor with 8 GB RAM it took approximately 18.2 Minutes to run through the 2000 generations.

The generated lengths of the bars of the mechanism are written in Table 5.1 and can there be compared to the Jansen mechanism. As seen in the third column of this table, which holds the differences of length to the Jansen mechanism, the value of a few genes varies more, which still results in a similar motion.

## 5. Results of the genetic algorithm

Holy numbers	genes	difference
$m^* = 15.00$	$a = 14.45$	-0.55
$b^* = 41.50$	$b = 41.04$	-0.46
$j^* = 50.00$	$c = 44.06$	-5.94
$n^* = 38.79$	$d = 36.59$	-2.20
$c^* = 39.30$	$e = 36.82$	-2.48
$k^* = 61.90$	$f = 57.80$	-4.10
$d^* = 40.10$	$g = 53.20$	13.10
$e^* = 55.80$	$h = 67.65$	11.85
$f^* = 39.40$	$i = 41.93$	2.53
$g^* = 36.70$	$j = 46.00$	9.30
$i^* = 49.00$	$k = 48.26$	-0.74
$h^* = 65.70$	$l = 72.12$	6.42
$x^* = 0.00$	$x_A = 3.01$	3.01
$y^* = 0.00$	$y_A = -3.98$	-3.98
$\gamma^* = 11.60^\circ$	$\gamma = 10.47^\circ$	-1.13°
with		
$l^* = 7.8$		
$a^* = 38.0$		

Table 5.1.: Best approximated mechanism to Jansen locus

In Figure 5.4 the newly generated mechanism can be compared to the Jansen mechanism, which is plotted in gray in the background. Due to the differences in length, the parts on the right hand side of the mechanism look like they are scaled up. The positioning of the fixed base, which is plotted in black, turned out to be very close to the one in the Jansen mechanism. The locus of the Jansen mechanism with the twelve target points is plotted in gray and the locus of the new mechanism is held in brown.

In Figure 5.5 an animation of the new mechanism is displayed. The step size of the crank is 30 degrees. The two mechanisms superpose well throughout the motion. The same animation is shown again in Fig. 5.6, although without the Jansen mechanism in the background, to exclusively see the motion of the new mechanism.

5. Results of the genetic algorithm

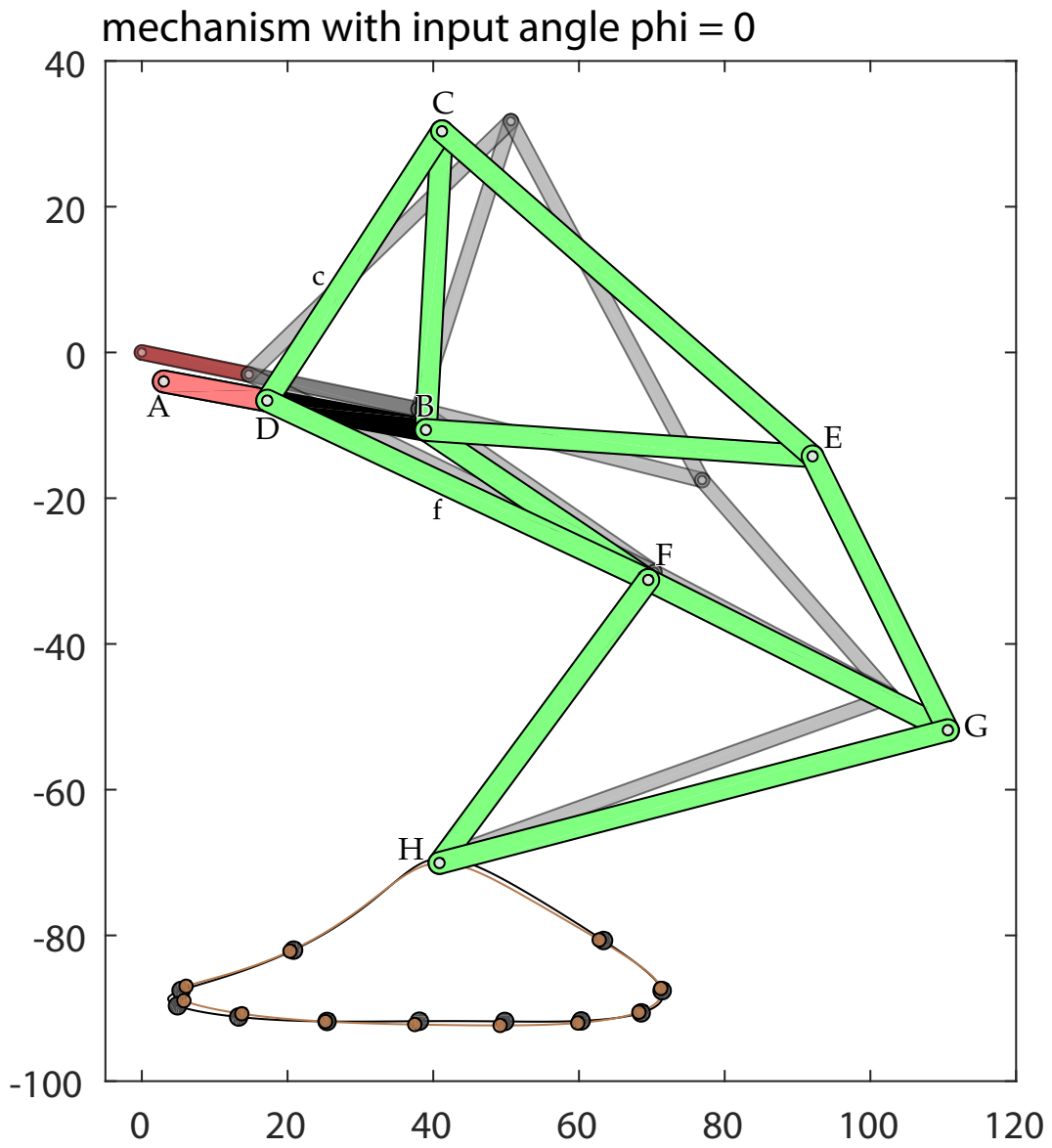


Figure 5.4.: New Jansen-style mechanism in comparison with the Jansen mechanism

## 5. Results of the genetic algorithm

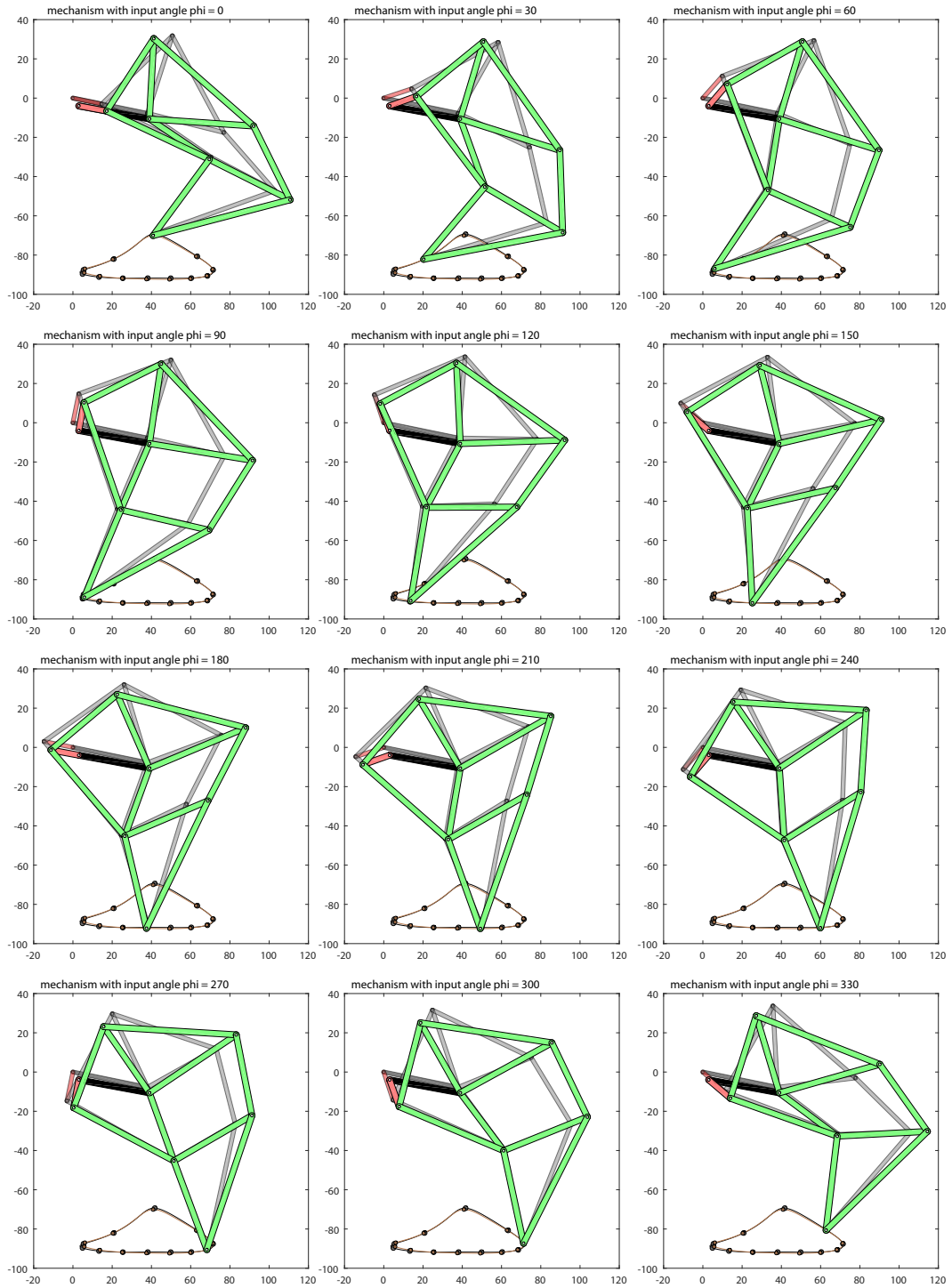


Figure 5.5.: Animation of the new mechanism in comparison to the Jansen mechanism

## 5. Results of the genetic algorithm

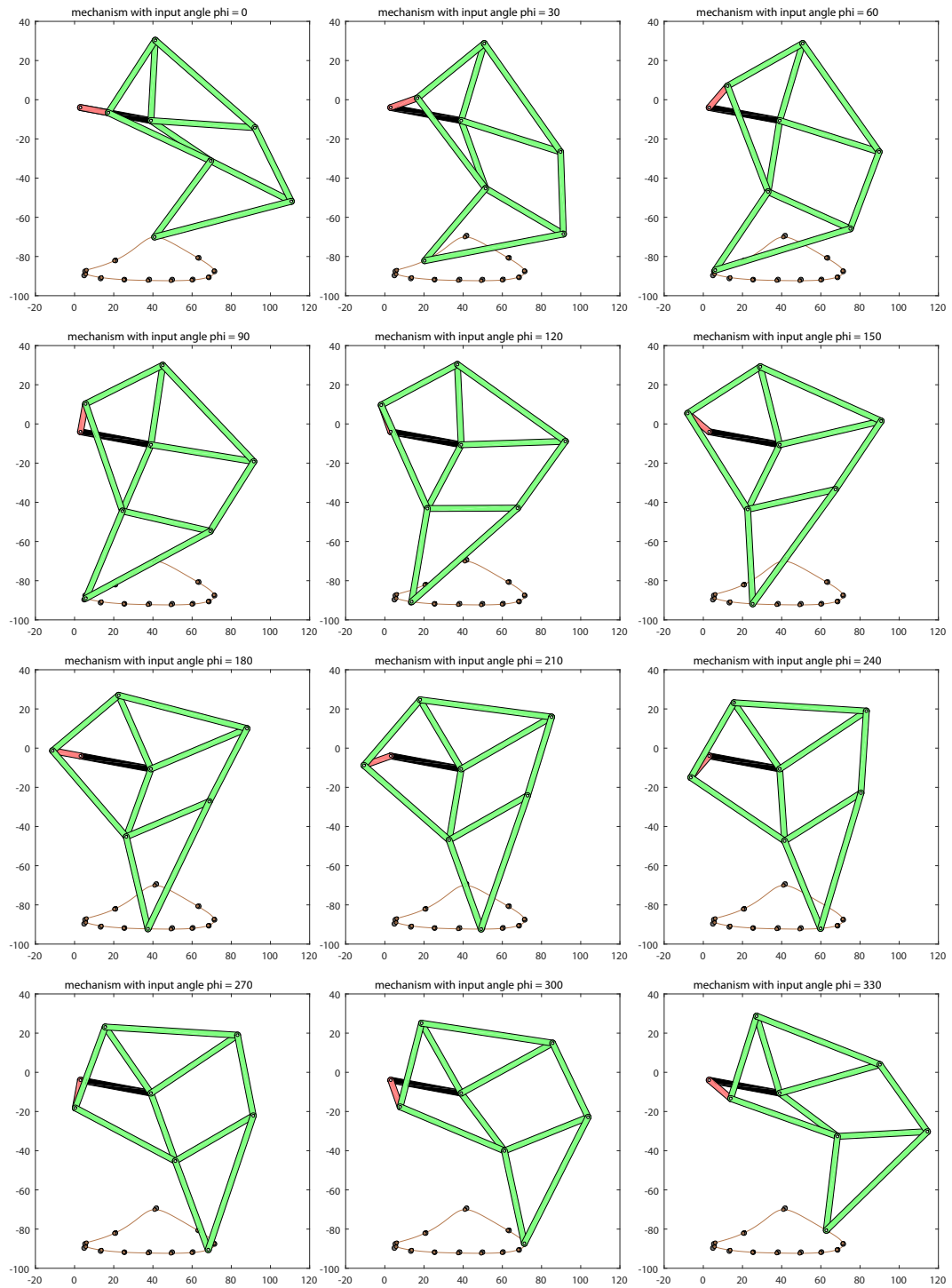
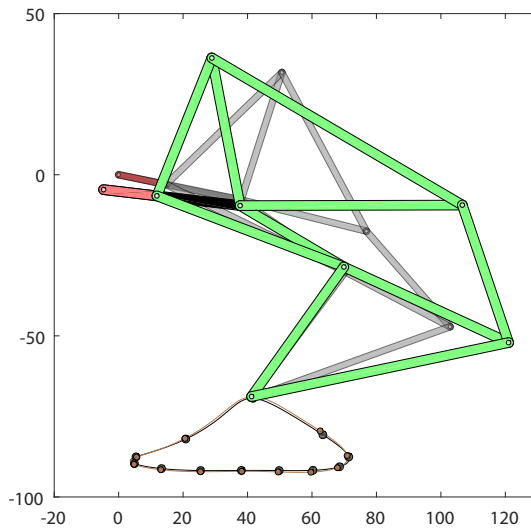


Figure 5.6.: Animation of the generated mechanism

## 5. Results of the genetic algorithm

### 5.1.1. Further results close to the Jansen mechanism



**parameters:**

$popsiz$  = 250,  $genmax$  = 1500,  $CP$  = 0.9,  $MP$  = 0.2,  $M$  = 0.25 and the allowed  $error = s/2 = 12/2 = 6$ .

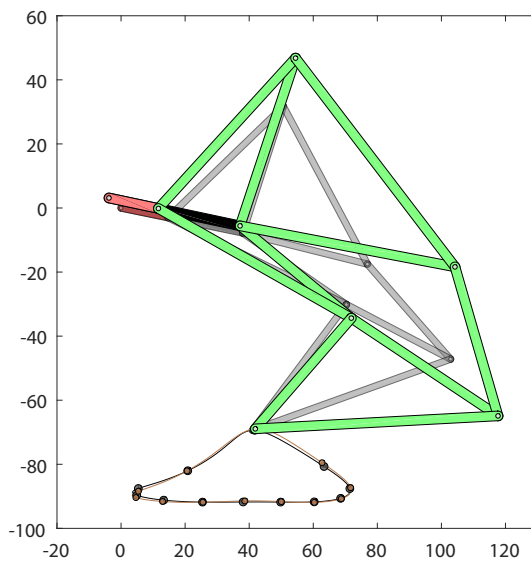
**generations:** 131

**remaining error:** 5.03

**run time:** approx. 1.1 min

**length of bars:**

$a = 16.66$ ,  $b = 46.65$ ,  $c = 46.06$ ,  
 $d = 42.67$ ,  $e = 37.40$ ,  $f = 62.08$ ,  
 $g = 68.95$ ,  $h = 90.15$ ,  $i = 45.02$ ,  
 $j = 56.25$ ,  $k = 49.36$ ,  $l = 81.49$ ,  
 $x_A = 1.40$ ,  $y_A = -4.62$ ,  $\gamma = 7.9^\circ$



**parameters:**

$popsiz$  = 250,  $genmax$  = 1000,  $CP$  = 0.9,  $MP$  = 0.2,  $M$  = 0.3 and the allowed  $error = s/2 = 12/2 = 6$ .

**generations:** 610

**remaining error:** 4.40

**run time:** approx. 4.3 min

**length of bars:**

$a = 15.78$ ,  $b = 55.14$ ,  $c = 63.52$ ,  
 $d = 41.84$ ,  $e = 45.11$ ,  $f = 69.26$ ,  
 $g = 68.29$ ,  $h = 81.98$ ,  $i = 48.42$ ,  
 $j = 55.04$ ,  $k = 45.73$ ,  $l = 75.87$ ,  
 $x_A = -3.77$ ,  $y_A = 3.13$ ,  $\gamma = 11.5^\circ$

### 5.2. Inverse mechanisms

The algorithm also delivered a type of mechanism, which is called *inverse mechanisms*. This category is classified and labeled due to an inverse or reverse look of the mechanism compared to the Jansen mechanism. When the angle of the crank regarding the fixed base is zero degrees, the two bars ( $c$  and  $f$ ) connected to the crank point to the left (see Fig. 5.7). This leads to a more compact mechanism although its motion when the crank is turned does not look as natural as the Jansen mechanisms. Another difference to the Jansen mechanism is that the lower triangle  $FGH$  with the foot tip  $H$  points towards the locus from the left. With approximately 44 % of all generated mechanisms, this type of mechanism made up the biggest group of the generated mechanisms.

The algorithm took 6.9 minutes to find the following mechanism with these parameters:

- $popsize = 250$ ,  $genmax = 1000$ ,  $CP = 0.9$ ,  $MP = 0.2$ ,  $M = 0.3$  and the allowed  $error = s/2 = 12/2 = 6$ .

The algorithm returned the following values for the length of the bars:

$$a = 15.86, b = 60.65, c = 41.58, d = 41.17, e = 50.46, f = 26.73, g = 31.61, \\ h = 88.18, i = 67.81, j = 14.51, k = 58.26, l = 50.55, x_A = -0.51, A = -20.74, \gamma = -18.9^\circ$$

This mechanism has a final error of 7.42, so the algorithm ran through all 1000 generations. On closer inspection, it is obvious to see that the bigger part of the error derives from the upper part of the locus, which is in general not as important.

In Figure 5.7 the inverse mechanism can be compared to the Jansen mechanism. Figure 5.8 shows the different look of the inverted mechanism compared to the Jansen mechanism during one full rotation of the crank. In Figure 5.9 an animation of the inverse mechanism is displayed.

## 5. Results of the genetic algorithm

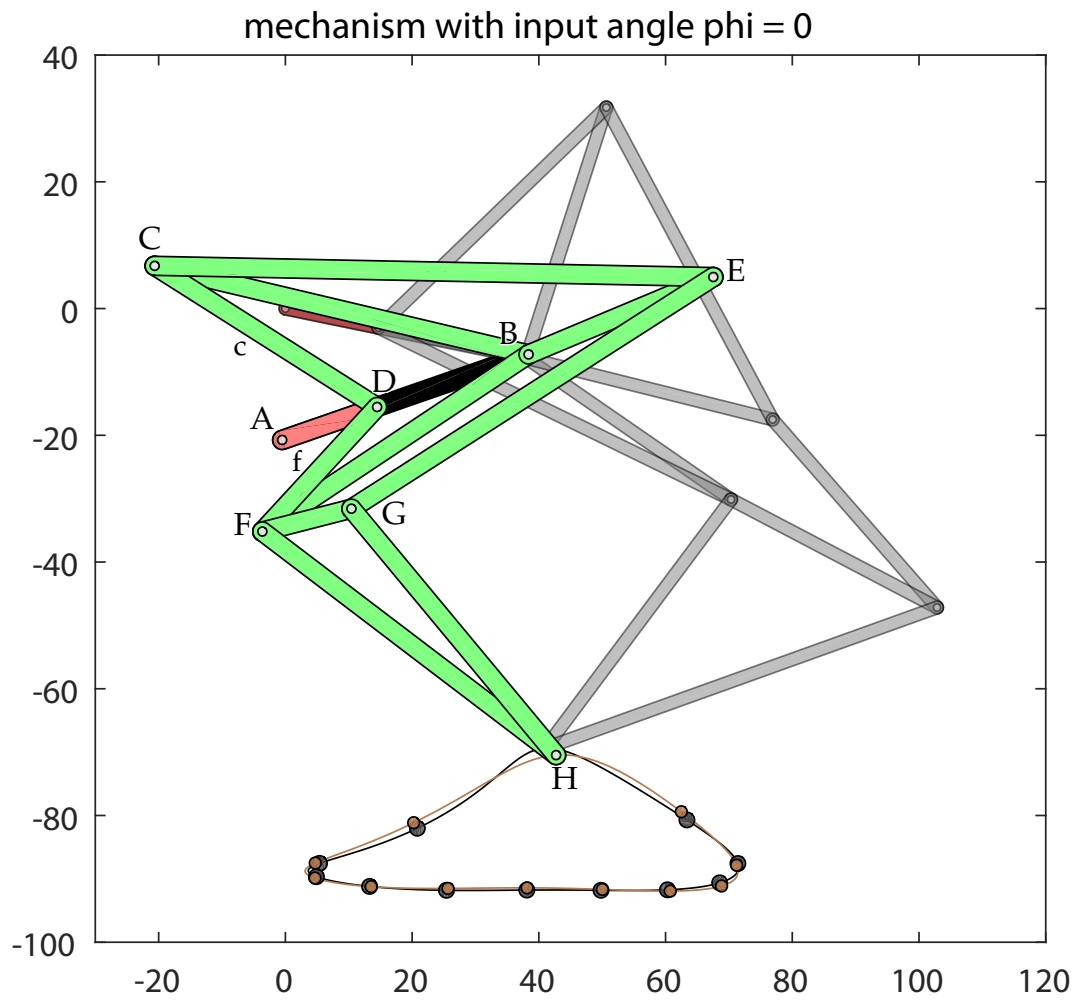


Figure 5.7.: Inverse mechanism in comparison with the Jansen mechanism

## 5. Results of the genetic algorithm

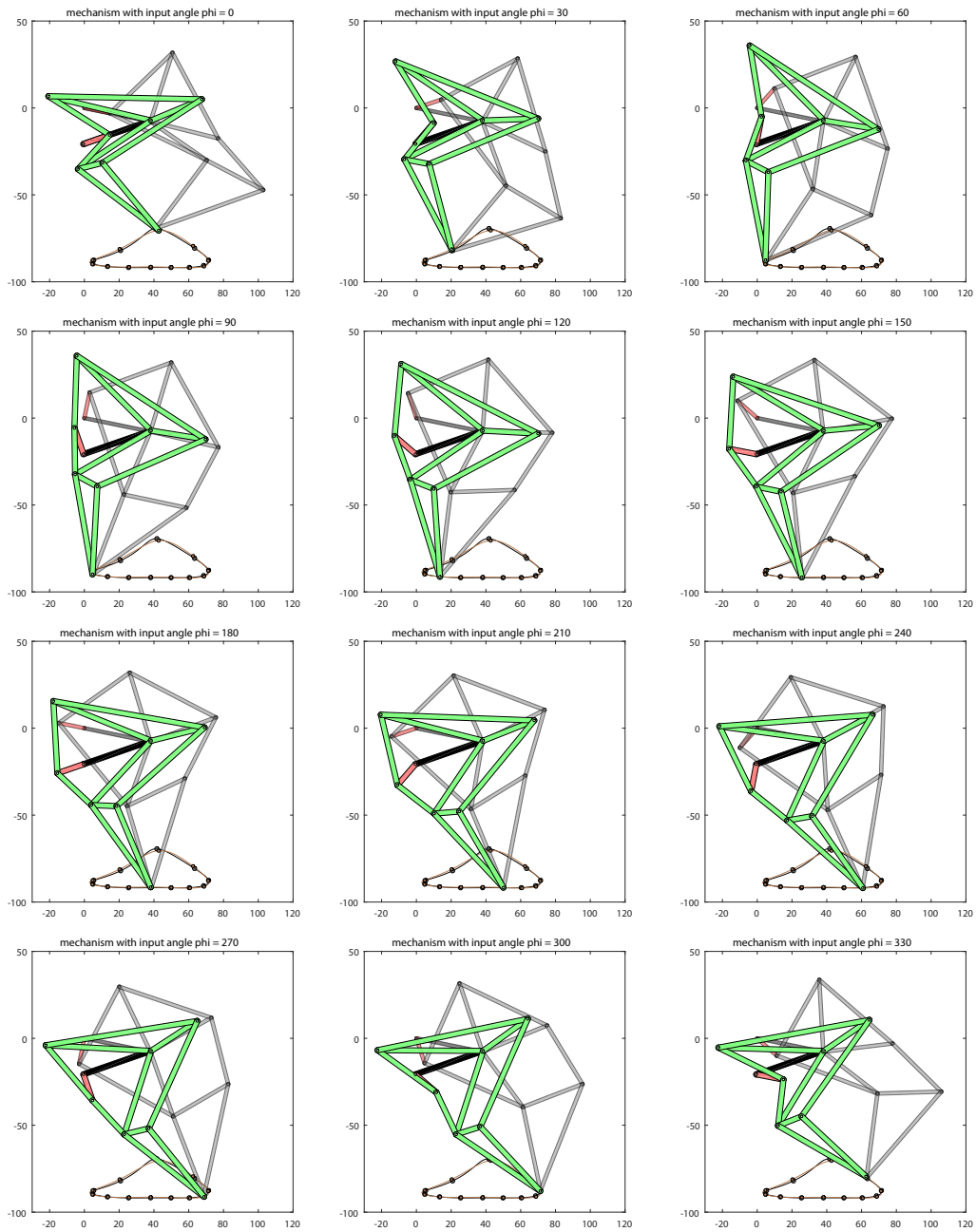


Figure 5.8.: Animation of the inverse mechanism in comparison to the Jansen mechanism

## 5. Results of the genetic algorithm

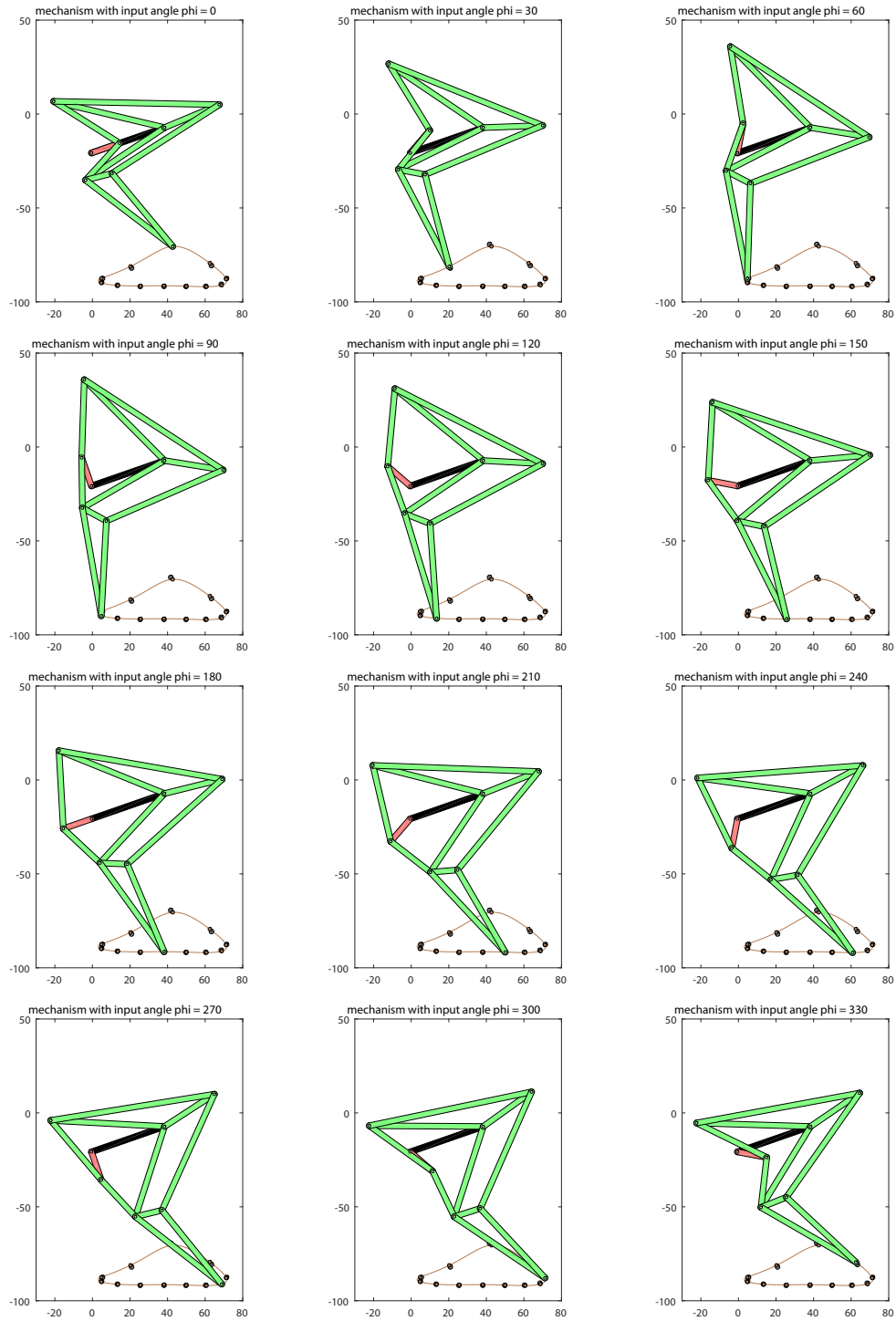
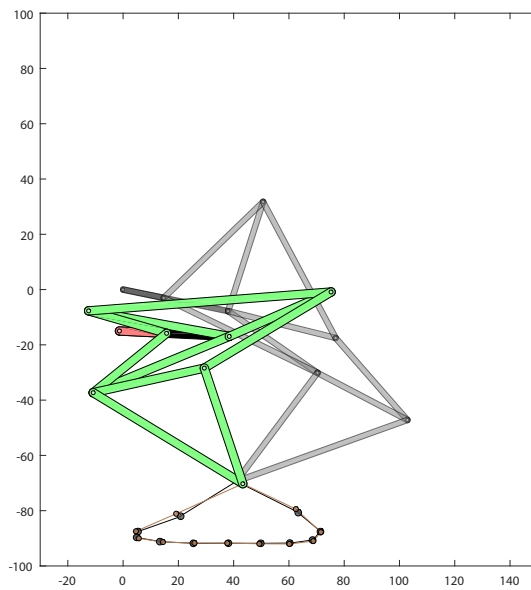


Figure 5.9.: Animation of the generated inverse mechanism

## 5. Results of the genetic algorithm

### 5.2.1. Further inverse results



**parameters:**

$popsize = 250$ ,  $genmax = 2000$ ,  $CP = 0.9$ ,  $MP = 0.3$ ,  $M = 0.15$  and the allowed error =  $s/12 = 12/12 = 1$ .

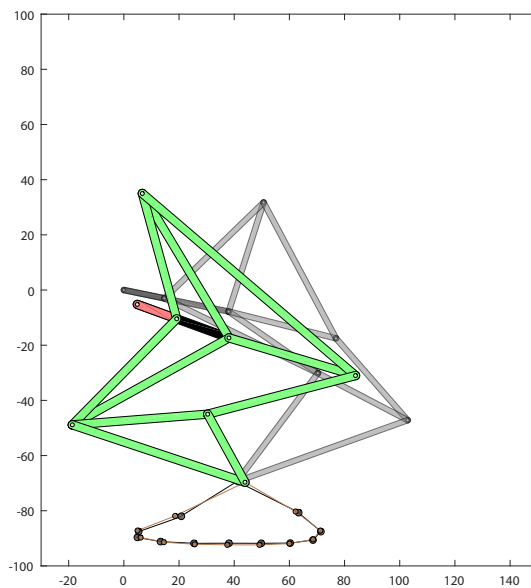
**generations:** 2000

**remaining error:** 12,74

**run time:** approx. 17.2 min

**length of bars:**

$a = 17.09$ ,  $b = 51.72$ ,  $c = 29.35$ ,  
 $d = 39.79$ ,  $e = 53.28$ ,  $f = 34.15$ ,  
 $g = 40.18$ ,  $h = 87.97$ ,  $i = 53.49$ ,  
 $j = 41.18$ ,  $k = 63.37$ ,  $l = 44.09$ ,  
 $x_A = -1.33$ ,  $y_A = -14.99$ ,  $\gamma = 2.9^\circ$



**parameters:**

$popsize = 250$ ,  $genmax = 2000$ ,  $CP = 0.8$ ,  $MP = 0.3$ ,  $M = 0.2$  and the allowed error =  $s/2 = 12/2 = 6$ .

**generations:** 2000

**remaining error:** 16,50

**run time:** approx. 17.8 min

**length of bars:**

$a = 15.20$ ,  $b = 61.03$ ,  $c = 47.11$ ,  
 $d = 35.36$ ,  $e = 64.93$ ,  $f = 53.93$ ,  
 $g = 47.87$ ,  $h = 101.62$ ,  $i = 55.39$ ,  
 $j = 49.20$ ,  $k = 65.94$ ,  $l = 28.14$ ,  
 $x_A = 4.88$ ,  $y_A = -5.22$ ,  $\gamma = 20.2^\circ$

### 5.3. Mixed mechanisms

This category of mechanisms is called *mixed mechanisms*. The main criteria for a mechanism to belong to this category are that either the bar with length represented by the genes  $c$  or  $f$  connected to the crank is pointing to the left and the other of these two bars is pointing to the right, when the crank is in the zero degree position. Only in 9 % of all mechanisms, this kind was developed.

With the following parameters a mechanism was generated:

- $popsize = 250$ ,  $genmax = 2000$ ,  $CP = 0.9$ ,  $MP = 0.3$ ,  $M = 0.12$  and the allowed  $error = 12/3 = 4$ .

The values for the length of the bars turned out to be  $a = 19.90$ ,  $b = 64.60$ ,  $c = 37.21$ ,  $d = 52.68$ ,  $e = 32.19$ ,  $f = 63.58$ ,  $g = 70.00$ ,  $h = 114.73$ ,  $i = 69.91$ ,  $j = 33.02$ ,  $k = 58.40$ ,  $l = 70.27$ ,  $x_A = -14.20$ ,  $y_A = -7.32$ ,  $\gamma = -1,7^\circ$  and the error was reduced to 6.1.

In Figure 5.10 the mixed mechanism can be compared to the Jansen mechanism. In Figure 5.11 the animation can be compared to the Jansen mechanism and in Figure 5.12 an animation of the mixed mechanism is displayed.

## 5. Results of the genetic algorithm

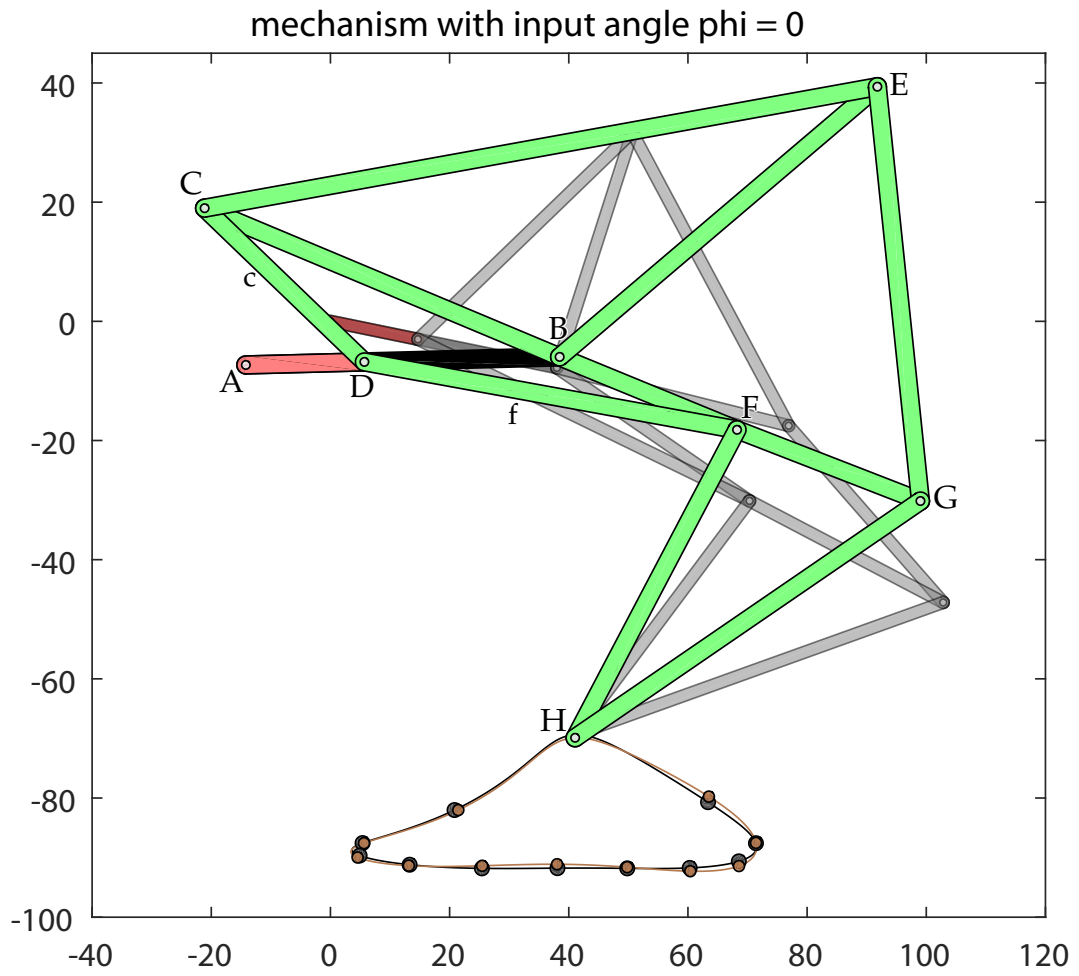


Figure 5.10.: Mixed mechanism in comparison with the Jansen mechanism

## 5. Results of the genetic algorithm

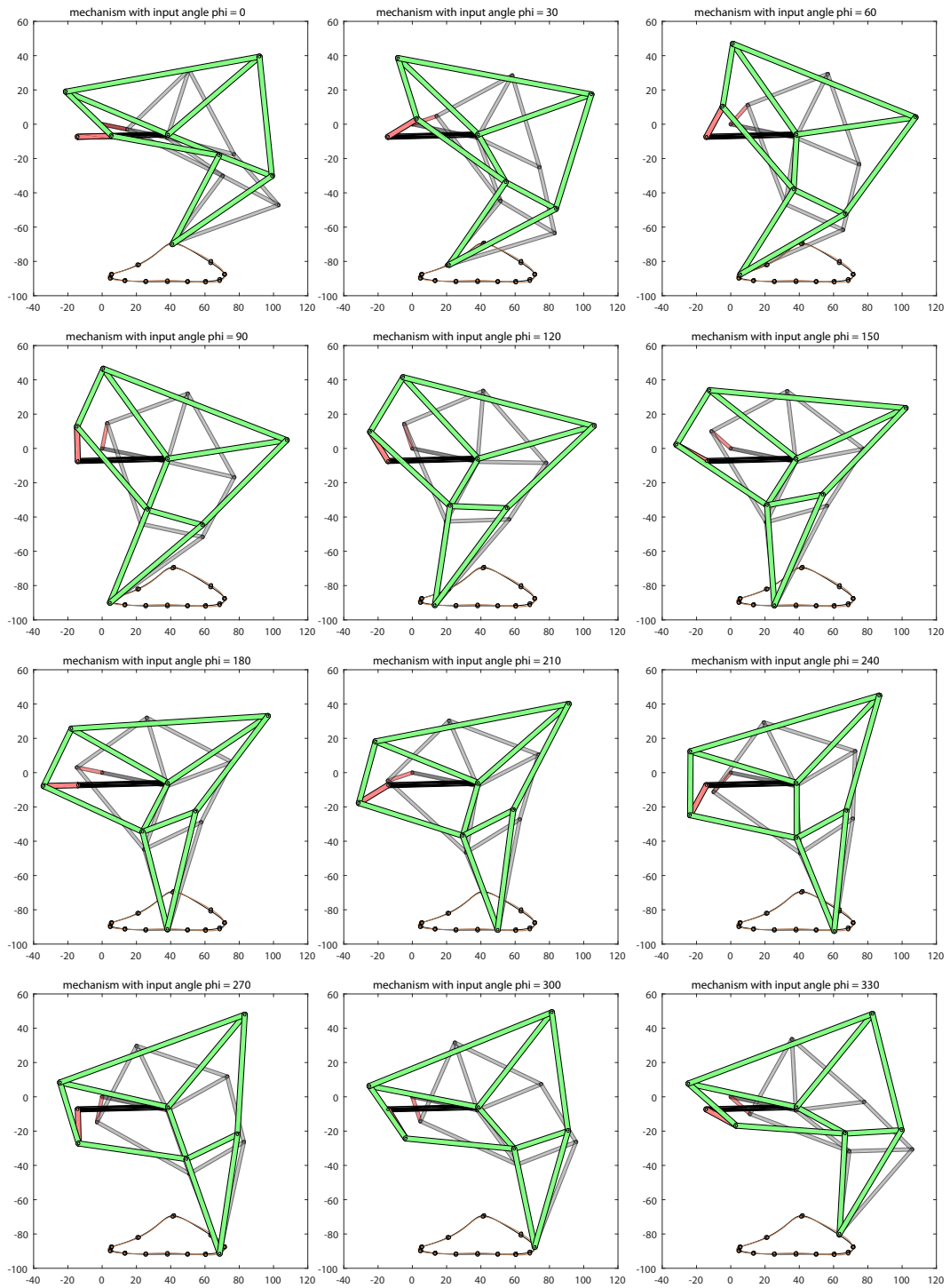


Figure 5.11.: Animation of the mixed mechanism in comparison to the Jansen mechanism

## 5. Results of the genetic algorithm

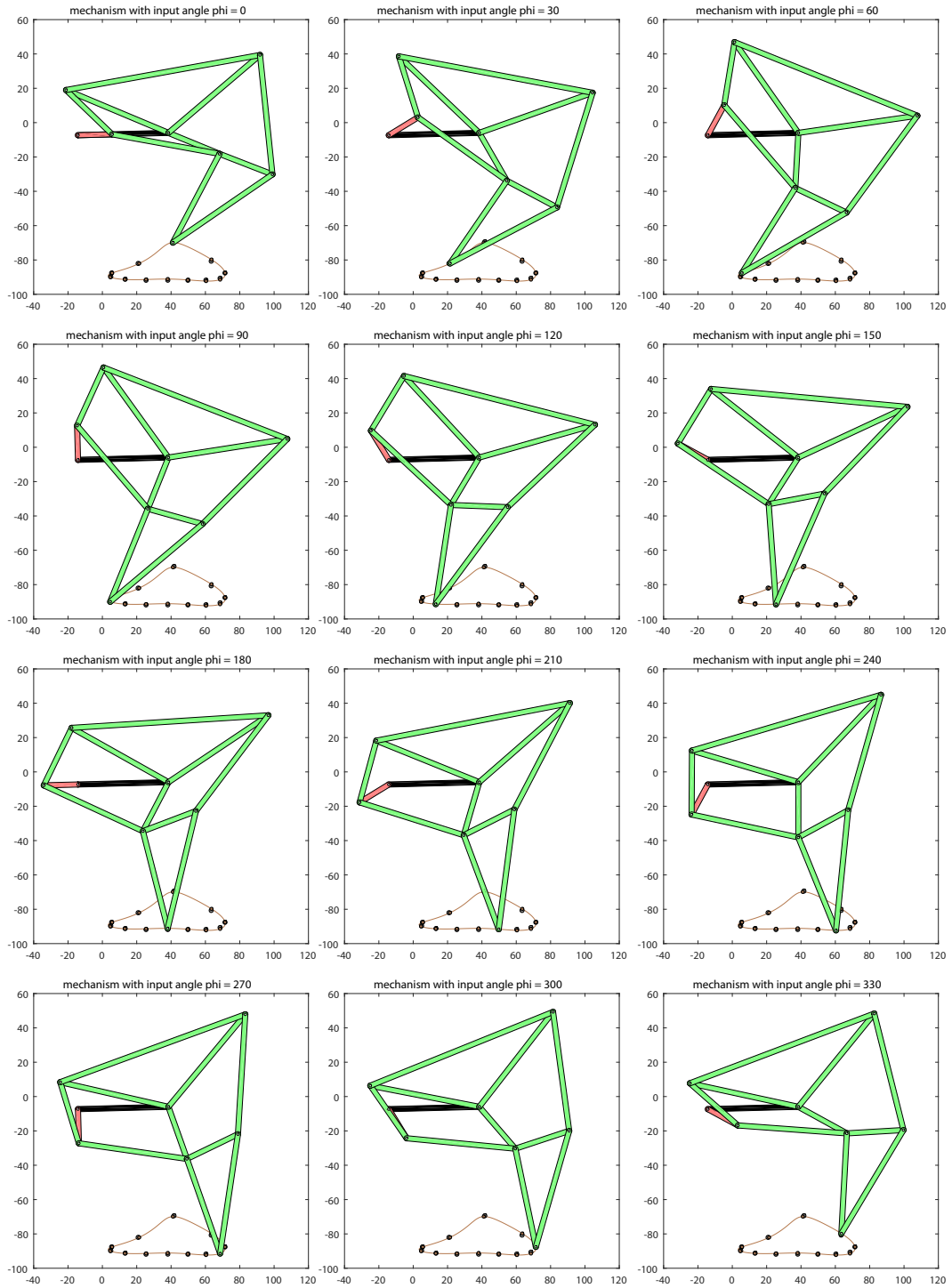
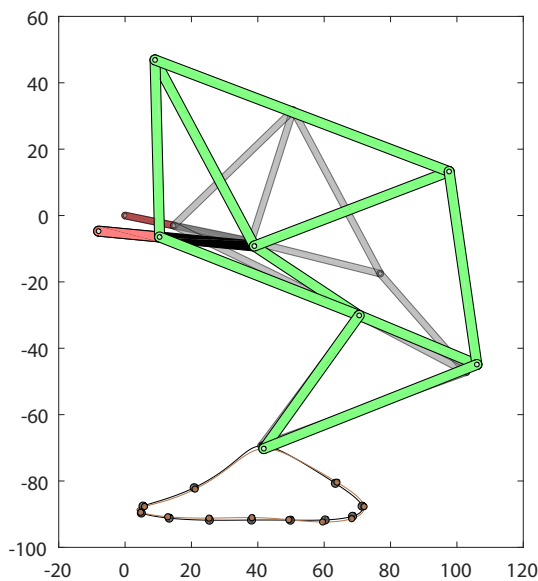


Figure 5.12.: Animation of the mixed mechanism

## 5. Results of the genetic algorithm

### 5.3.1. Further mixed results



**parameters:**

$popsize = 250$ ,  $genmax = 1500$ ,  $CP = 0.9$ ,  $MP = 0.2$ ,  $M = 0.25$  and the allowed error  $= s/2 = 12/2 = 6$ .

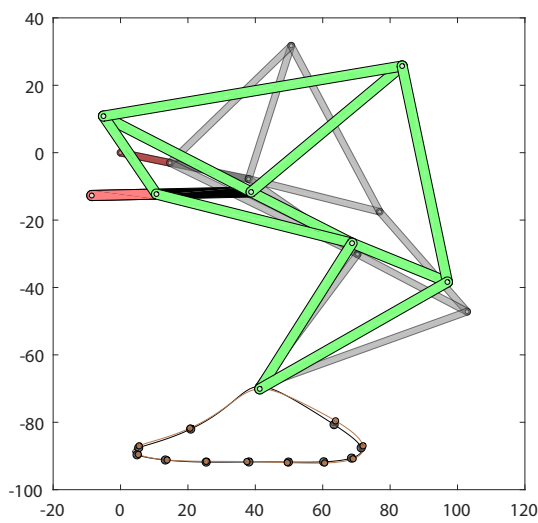
**generations:** 787

**remaining error:** 5.12

**run time:** approx. 5.9 min

**length of bars:**

$a = 18.46$ ,  $b = 63.57$ ,  $c = 53.37$ ,  
 $d = 47.15$ ,  $e = 37.88$ ,  $f = 64.63$ ,  
 $g = 62.84$ ,  $h = 94.79$ ,  $i = 58.75$ ,  
 $j = 38.43$ ,  $k = 49.36$ ,  $l = 69.03$ ,  
 $x_A = -7.98$ ,  $y_A = -4.71$ ,  $\gamma = 10.9^\circ$



**parameters:**

$popsize = 250$ ,  $genmax = 1500$ ,  $CP = 0.9$ ,  $MP = 0.2$ ,  $M = 0.25$  and the allowed error  $= s/2 = 12/2 = 6$ .

**generations:** 666

**remaining error:** 4.73

**run time:** approx. 4.5 min

**length of bars:**

$a = 19.20$ ,  $b = 49.25$ ,  $c = 27.97$ ,  
 $d = 47.29$ ,  $e = 33.59$ ,  $f = 59.85$ ,  
 $g = 58.36$ ,  $h = 89.87$ ,  $i = 65.48$ ,  
 $j = 30.55$ ,  $k = 51.17$ ,  $l = 64.08$ ,  
 $x_A = -8.53$ ,  $y_A = -12.71$ ,  $\gamma = -1.2^\circ$

## 5.4. Infeasible mechanisms

In Figure 5.13 an infeasible result of the algorithm can be seen. Approximately 20 % of all generated mechanisms turned out to be unusable. The main criterion for usability was that the foot tip  $H$  always has to be the lowest point of the mechanism. An example was created with the following parameters:

- $popsize = 250$ ,  $genmax = 2000$ ,  $CP = 0.8$ ,  $MP = 0.3$ ,  $M = 0.2$  and the allowed  $error = 12/4 = 3$ .

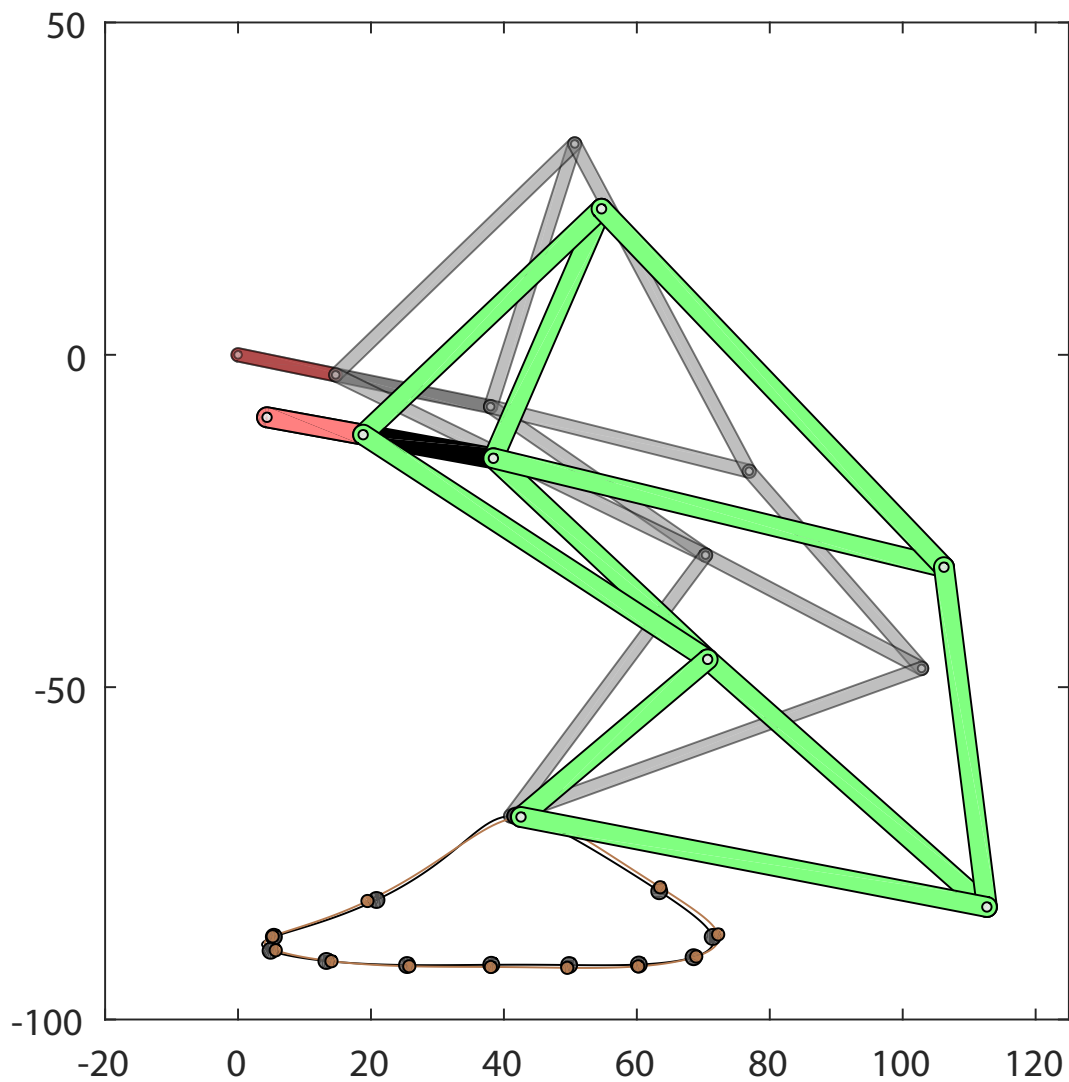


Figure 5.13.: Infeasible mechanism in comparison with the Jansen mechanism

## 6. Conclusion

In hindsight, the genetic algorithm was a good choice to synthesize Jansen-style mechanisms to a given locus. The development of the starting population turned out to be the most challenging part of the algorithm.

The approach in this paper was successful in finding numerous mechanisms which met our requirements. With the used constraints although, Jansen's *twelve holy numbers* were not reproducible. With identical inputs a great variety of results was produced, which could be categorized into four groups. The approximate percentage on how often a specific type of mechanism was produced can be seen in Figure 6.1.

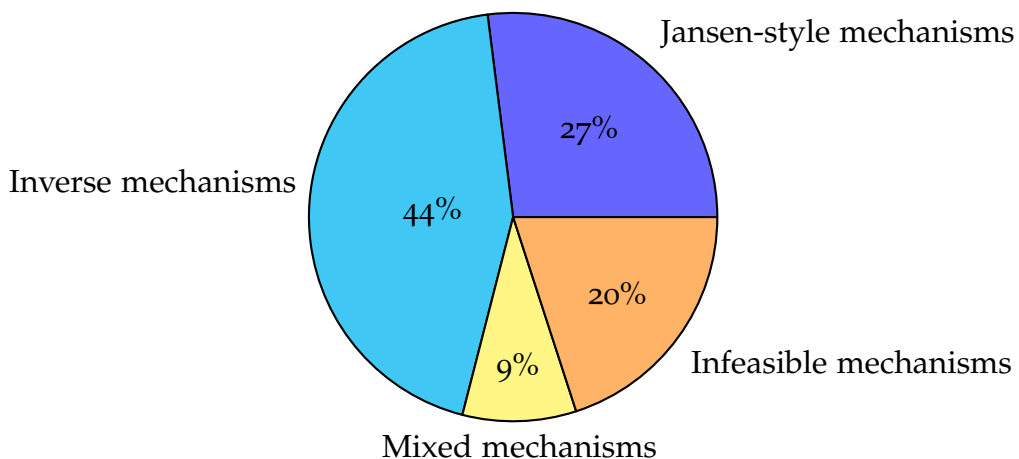


Figure 6.1.: Percentage of the produced types of mechanisms

In order to find a mechanism for a specific purpose, the algorithm would have to be run through several times. One very interesting aspect of the results were the categories of the *inverse* and *mixed* mechanism. These had not been expected. The inverse mechanisms have a more compact shape and the tip of the foot reaches the locus from the other side. This could eventually be used for specified applications. Some of the mixed mechanisms turned out to be low in height in terms of height comparison with the Jansen mechanism. For some purposes this could be an advantage.

## 6. Conclusion

Unfortunately approximately 20 % of the generated mechanisms were infeasible, meaning that the foot tip of the mechanisms was not the lowest part of the mechanism. It would have been a lot of work to avoid this category. Many mechanisms would have to be deleted, since this only is noticeable until a couple of generations have passed. This effort would have been out of the scope of this thesis. Inverse or mixed mechanisms could be eliminated more easily, but since they are an interesting output, these results were kept in the algorithm.

In roughly 18 % of all run tests the algorithm stopped because the allowed error was reached. Within these tests only mechanisms of the categories close to the Jansen mechanism, mixed mechanisms and infeasible mechanisms were produced. Slightly more than 52 % of all mechanisms close to the Jansen mechanism were generated before the maximum allowed number of generations was reached. The inverse mechanisms are the most common output, but they seem to converge slower.

## References

- [1] J.A. Cabrera, A. Simon, and M. Prado. "Optimal synthesis of mechanisms with genetic algorithms." In: *Mechanism and Machine Theory* 37.10 (2002), pp. 1165–1177. ISSN: 0094-114X.
- [2] A. Gferrer. *Kinematik und Robotik*. 2008.
- [3] T. Jansen. *The Great Pretender*. 010 Publishers, 2007. ISBN: 9789064506307.
- [4] H. Leopoldseder, C. Schöpf, and G. Stocker. *The network for art, technology and society: the first 30 years ; Ars Electronica 1979-2009*. Distributed Art Pub Incorporated, 2009. ISBN: 9783775725231.
- [5] Kumara Sastry, David Goldberg, and Graham Kendall. "Genetic Algorithms." In: *Search Methodologies: Introductory Tutorials in Optimization and Decision Support Techniques*. Ed. by Edmund K. Burke and Graham Kendall. Boston, MA: Springer US, 2005, pp. 97–125. ISBN: 978-0-387-28356-2.
- [6] *Theo Jansen's Strandbeest website*. URL: [http://www.strandbeest.com/theo\\_cv.php](http://www.strandbeest.com/theo_cv.php) (visited on 02/18/2018).
- [7] W. Wunderlich. *Ebene Kinematik*. Bibliographisches Institut, 1970. ISBN: 1677839414.